Chapter 7

Analysis of unsteady two-phase peristaltic flow in a tube of exponentially changing cross sectional area: Application to sliding hiatus hernia

7.1 Introduction

Peristalsis is the predominant mechanism of pumping within the bodies of humans and animals. Unlike piston pumps used in engineering applications, the combination of the sequence of alternative contractions and relaxations of the

vessel-wall due to the propagation of waves makes it unique. The wave generation is a reflex phenomenon and is made up of longitudinal and circular muscles of the tubular vessel.

Oesophagus is one of such vessels where transportation is due to peristalsis. Under normal conditions, the oesophagus is a uniform circular cylindrical tube. But whenever the abdomen protrudes through the hiatus, the oesophagus dysfunctions and the oesophagus is dimensionally changed. This disorder is called hiatal herniation in medical science.

Hiatal hernia is of two types: one of them is sliding hiatal hernia which has some symptoms but is not a serious dysfunction as it discovers normalcy soon after protrusion while the other one, known as para-hiatal hernia, is a serious case and needs clinical correction. In case of sliding hiatal hernia, the oesophagus may be somewhere diverging and converging somewhere else or may be a combination of the two. Pandey and Singh (2019) investigated the flow of Herschel-Bulkley fluids in tubes of variable cross-section with application to sliding hiatal hernia.

The intake in oesophagus may be purely water but mostly it is a mixture of fluid and solid particles. Such a swallowing was modelled by Pandey and Singh (2018) for a uniform tube based on Drew's model (1979) for particle-fluid suspension by using a perturbation technique. Drew [(1979), (1983)] had presented a two-phase flow model and discussed the stability of a Stokes layer of a particle-fluid mixture. The wall equation they considered was the one formulated theoretically by Pandey *et al.* (2017) in which the wave amplitude increases while propagating to match the high pressure in the distal oesophagus. The fact was experimentally discovered by Kahrilas *et al.* (1995).

The inferences drawn by Pandey and Singh (2018) are useful. They contradicted previous conclusions [Srivastava and Srivastava (1989), Misra and Pandey (1994)] and propounded that solid particles move faster than the fluid near the boundary of the vessel while they are slower than the fluid away from the boundary, which conforms the physics of such a flow. This is due to the fact that no-slip condition cannot be used on solid particles. However, due to the complexity involved, the series solutions were restricted to the first order of the perturbation parameter.

Apart from experimental investigation of the two-dimensional peristaltic flow of solid particles with different geometries initiated by Hung and Brown (1976), a similar theoretical study of the particle-fluid suspension was done by Srivastava and Srivastava (1989) who reported that the critical reflux pressure is lower for the particle-fluid suspension than that for the particle-free fluid. It is further observed that the mean flow reversal is strongly dependent on the particle concentration and the presence of particles in the fluid favours reversal of flow. Misra and Pandey (1994) subsequently studied axisymmetric flows. Jimenez-Lozano *et al*. (2011) presented an analysis of the axisymmetric peristaltic flow of a solid-liquid mixture in order to investigate the mechanics of ureteral peristalsis in the presence of solid particles as in ureteral lithiasis. Mekheimer (2008) theoretically analyzed peristaltic motion of a particle-fluid suspension through a uniform and non-uniform annulus. Some recent publications discussing different aspects based on Drew's model are worth mentioning [Bhatti and Zeeshan (2016), Bhatti *et al*. (2016a, 2017b, 2017c, 2018d, 2016e), Zeeshan *et al*. (2017)].

Pandey and Singh (2019), who tried to study sliding hiatal hernia, investigated the flow of Herschel-Bulkley fluids in tubes of variable cross-section. In case of cross sectional changes, we generally consider divergence or convergence

of a tube of linear nature. However, such biological tissues altered in shape are generally not linear. The new shape may be fitted with an exponential curve. Therefore an exponential shape for modelling seems to be more appropriate.

We plan to construct a mathematical model for hiatal hernia. With the considerations in the discussion given above, we investigate the unsteady flow of solid particles suspended in a Newtonian fluid through a tube with exponentially varying cross sectional area by duly considering the convective acceleration terms. The flow is induced by peristaltic waves of dilating amplitude formulated by Pandey *et al.* (2017). The perturbation solution too involves higher order terms.

7.2 Mathematical Formulation

We consider an axisymmetric flow of a mixture of small solid particles and an incompressible Newtonian viscous fluid in a circular cylindrical tube whose cross-sectional area changes with its length.

Oesophageal wall equation given by Pandey *et al.* (2017) requires some modification as given below to incorporate exponential change in the cross section along the tube length:

$$\tilde{h}(\tilde{x},\tilde{\omega},\tilde{t}) = ae^{\tilde{b}\tilde{x}} - \tilde{\phi}\, e^{\tilde{\omega}\tilde{x}} \cos^2 \frac{\pi}{\lambda}(\tilde{x} - c\tilde{t}), \tag{7.1}$$

where $\tilde{h}$, $\tilde{x}$, $\tilde{t}$, a, $\tilde{b}$, $\tilde{\phi}$, $\tilde{\omega}$, λ and c are the radial displacement of the wall, axial coordinate, time, the radius of the tube, the tube gradient parameter which changes the cross section depending on the length of the tube, wave amplitude,

the wave amplitude dilation parameter, the wavelength and the wave velocity respectively.

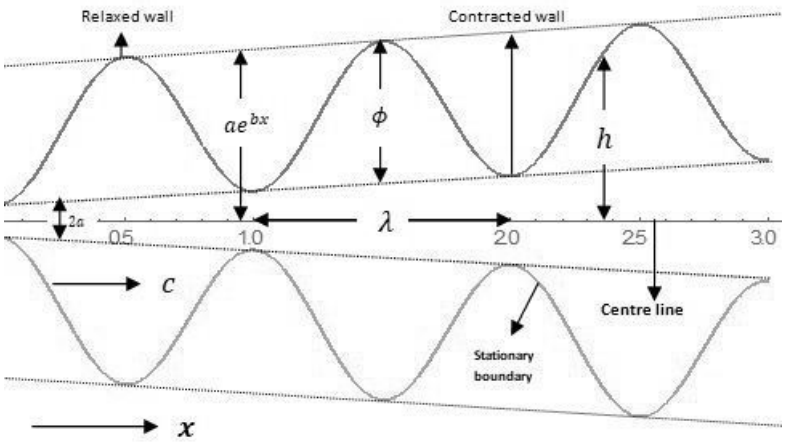

Figure 7.1: Schematic diagram of wall positions of oesophagus, based on the equation (7.9), when a peristaltic wave of slightly dilating amplitude propagates along it with velocity c.

The following are the governing equations of the two-phase unsteady flow due to Drew [1979] in the cylindrical polar coordinates:

Fluid phase:

$$\frac{\partial}{\partial \tilde{x}}[(1-C)\tilde{u}_f] + \frac{1}{\tilde{r}}\frac{\partial}{\partial \tilde{r}}[(1-C)\tilde{r}\tilde{v}_f] = 0, \tag{7.2}$$

$$\rho_f(1-C)\left(\frac{\partial \tilde{v}_f}{\partial \tilde{t}} + \tilde{u}_f\frac{\partial \tilde{v}_f}{\partial \tilde{x}} + \tilde{v}_f\frac{\partial \tilde{v}_f}{\partial \tilde{r}}\right) = -(1-C)\frac{\partial \tilde{p}}{\partial \tilde{r}} + \mu_s(C)(1-C)\left\{\frac{\partial^2 \tilde{v}_f}{\partial \tilde{x}^2} + \frac{\partial}{\partial \tilde{r}}\left(\frac{1}{\tilde{r}}\frac{\partial(\tilde{r}\tilde{v}_f)}{\partial \tilde{r}}\right)\right\} + CS(\tilde{v}_p - \tilde{v}_f), \tag{7.3}$$

$$\rho_f(1-C)\left(\frac{\partial \tilde{u}_f}{\partial \tilde{t}}+\tilde{u}_f\frac{\partial \tilde{u}_f}{\partial \tilde{x}}+\tilde{v}_f\frac{\partial \tilde{u}_f}{\partial \tilde{r}}\right)=-(1-C)\frac{\partial \tilde{p}}{\partial \tilde{x}}+\mu_s(C)(1-C)\left\{\frac{\partial^2 \tilde{u}_f}{\partial \tilde{x}^2}+\frac{1}{\tilde{r}}\frac{\partial}{\partial \tilde{r}}\left(\tilde{r}\frac{\partial \tilde{u_f}}{\partial \tilde{r}}\right)\right\}+CS(\tilde{u_p}-\tilde{u_f}), \quad (7.4)$$

Particulate phase

$$\frac{\partial}{\partial \tilde{x}}(C\tilde{u}_p)+\frac{1}{\tilde{r}}\frac{\partial}{\partial \tilde{r}}(C\tilde{r}\tilde{v}_p)=0, \quad (7.5)$$

$$\rho_p C\left(\frac{\partial \tilde{v}_p}{\partial \tilde{t}}+\tilde{u}_p\frac{\partial \tilde{v}_p}{\partial \tilde{x}}+\tilde{v}_p\frac{\partial \tilde{v}_p}{\partial \tilde{r}}\right)=-C\frac{\partial \tilde{p}}{\partial \tilde{r}}+CS(\tilde{v_f}-\tilde{v_p}), \quad (7.6)$$

$$\rho_p C\left(\frac{\partial \tilde{u}_p}{\partial \tilde{t}}+\tilde{u}_p\frac{\partial \tilde{u}_p}{\partial \tilde{x}}+\tilde{v}_p\frac{\partial \tilde{u}_p}{\partial \tilde{r}}\right)=-C\frac{\partial \tilde{p}}{\partial \tilde{x}}+CS(\tilde{u_f}-\tilde{u_p}), \quad (7.7)$$

where $\tilde{u}_f$, $\tilde{v}_f$, $\tilde{u}_p$, $\tilde{v}_p$, ρ_f, ρ_p, C, $\rho_f(1-C)$, $\rho_p C$, $\tilde{p}$, and $\mu_s(C)$ represent respectively axial velocity of the fluid phase, radial velocity of the fluid phase, axial velocity of the particulate phase, radial velocity of the particulate phase, actual density of the fluid, actual density of the particulate material, volume fraction of the solid particles in the mixture, the fluid phase density, the particle phase density, pressure, drag coefficient of the interaction for the force exerted by one phase on the other and the effective viscosity of suspension.

For the present problem, the expression for the drag coefficient for a small particle at low Reynolds number, $S = (9\mu_0)/(4{r_p}^2)$, and Einstein's formula, $\mu_e = \mu_0\,\mu_r$, will be used, where μ_0 is the viscosity of fluid, r_p is the radius of particle and $\mu_r(C) = 1 + 5/2C$, [Mekheimer *et al.* (2008)].

For the further analysis, the dimensionless parameters are introduced as follows:

$$\begin{aligned} x =& \frac{\tilde{x}}{\lambda}, r = \frac{\tilde{r}}{a}, t = \frac{c\tilde{t}}{\lambda}, u_f = \frac{\tilde{u_f}}{c}, v_f = \frac{\tilde{v_f}}{c\delta}, u_p = \frac{\tilde{u_p}}{c}, \\ v_p =& \frac{\tilde{v_p}}{c\delta}, \delta = \frac{a}{\lambda}, h = \frac{\tilde{h}}{a}, b = \tilde{b}\lambda, \rho = \frac{\rho_p}{\rho_f}, \phi = \frac{\tilde{\phi}}{a}, \\ p =& \frac{\tilde{p}a\delta}{\mu_s c}, Re_0 = \frac{ac\rho_f}{\mu_0}, Q = \frac{\tilde{Q}}{\pi a^2 c}, \omega = \tilde{\omega}\lambda, Re = \delta Re_0, M = \frac{9}{4}\left(\frac{a}{r_p}\right)^2 \end{aligned} \tag{7.8}$$

where δ, Re_0, Re and M are respectively the wave number, the Reynolds number, the modified Reynolds number and the drag parameter.

In terms of these non-dimensional quantities reduce the wall equation (7.1) and governing equations (7.2)-(7.7) to

$$h(x, \omega, t) = e^{bx} - \phi\, e^{\omega x} \cos^2 \pi(x - t), \tag{7.9}$$

$$\frac{\partial}{\partial x}[(1 - C)u_f] + \frac{1}{r}\frac{\partial}{\partial r}[(1 - C)rv_f] = 0, \tag{7.10}$$

$$\begin{aligned} \delta^3 Re_0(1 - C)\left(\frac{\partial v_f}{\partial t} + u_f\frac{\partial v_f}{\partial x} + v_f\frac{\partial v_f}{\partial r}\right) = -\mu_r(1 - C)\frac{\partial p}{\partial r} + \mu_r(1 - C)\left\{\delta^4\frac{\partial^2 v_f}{\partial x^2}\right. \\ \left. + \delta^2\frac{\partial}{\partial r}\left(\frac{1}{r}\frac{\partial(rv_f)}{\partial r}\right)\right\} + \delta^2 CS(v_p - v_f), \end{aligned} \tag{7.11}$$

$$\delta Re_0(1-C)\left(\frac{\partial u_f}{\partial t}+u_f\frac{\partial u_f}{\partial x}+v_f\frac{\partial u_f}{\partial r}\right)=-\mu_r(1-C)\frac{\partial p}{\partial x}+\mu_r(1-C)\left\{\delta^2\frac{\partial^2 u_f}{\partial x^2}+\frac{1}{r}\frac{\partial}{\partial r}\left(r\frac{\partial u_f}{\partial r}\right)\right\}+CM(u_p-u_f), \quad (7.12)$$

$$\frac{\partial}{\partial x}(Cu_p)+\frac{1}{r}\frac{\partial}{\partial r}(Crv_p)=0, \quad (7.13)$$

$$\rho CRe_0\delta^3\left(\frac{\partial v_p}{\partial t}+u_p\frac{\partial v_p}{\partial x}+v_p\frac{\partial v_p}{\partial r}\right)=-C\mu_r\frac{\partial p}{\partial r}+CM\delta^2(v_f-v_p), \quad (7.14)$$

$$\rho CRe_0\delta\left(\frac{\partial u_p}{\partial t}+u_p\frac{\partial u_p}{\partial x}+v_p\frac{\partial u_p}{\partial r}\right)=-C\mu_r\frac{\partial p}{\partial x}+CM(u_f-u_p). \quad (7.15)$$

For achieving a useful solution of a system of differential equations, boundary conditions are required. However, in a practical scenario such as one undertaken here solid particles and physics of fluid have to be perfectly appropriate. For example, no solid particle can stick to a solid boundary otherwise the definition of rigidity will be violated. Actually, it is dragged by the fluid which sticks to the boundary. Therefore, we cannot impose the no-slip condition on the solid particles at the tubular wall. The non-dimensional boundary conditions, to be introduced on the fluid particles and solid particles for the sake of solution of the problem may be put as follows.

$$
\begin{aligned}
u_f &= 0 \text{ at } r = h, \ \frac{\partial u_f}{\partial r} = 0 \text{ at } r = 0, \\
v_f &= 0 \text{ at } r = 0, v_f = \frac{\partial h}{\partial t} \text{ at } r = h, \\
\frac{\partial u_p}{\partial_r} &= 0, \text{at } r = 0, v_p = 0 \text{ at } r = 0.
\end{aligned} \tag{7.16}
$$

7.3 Method of Solution

A regular perturbation technique is used to analyze the problem and get a series solution in terms of the wave number δ. Following Jimenez-Lozano (2011), we introduce the wave number $\delta << 1$ and consider that the particle volume fraction C is of the form $C = \delta C^{(1)}$ and hence very small. Further, we seek series solutions for the fluid velocities (u_f, v_f), solid particle velocities (u_p, v_p) and the pressure p as well of the form

$$u_f(x,r,t) = {u_f}^{(0)} + \delta {u_f}^{(1)} + \delta^2 {u_f}^{(2)} + ..., \tag{7.17}$$

$$v_f(x,r,t) = {v_f}^{(0)} + \delta {v_f}^{(1)} + \delta^2 {v_f}^{(2)} + ..., \tag{7.18}$$

$$u_p(x,r,t) = {u_p}^{(0)} + \delta {u_p}^{(1)} + \delta^2 {u_p}^{(2)} + ..., \tag{7.19}$$

$$v_p(x,r,t) = {v_p}^{(0)} + \delta {v_p}^{(1)} + \delta^2 {v_p}^{(2)} + ..., \tag{7.20}$$

$$p(x,r,t) = p^{(0)} + \delta p^{(1)} + \delta^2 p^{(2)} + ... \tag{7.21}$$

Substituting the series forms given in equations (7.17)-(7.21) into the governing equations (7.10)-(7.15), and then collecting terms of like powers of δ on the two sides, the equations are reduced to a set of linear equations as given

below:

Zeroth order:

$$\frac{\partial}{\partial x}[{u_f}^{(0)}] + \frac{1}{r}\frac{\partial}{\partial r}[r{v_f}^{(0)}] = 0, \tag{7.22}$$

$$\frac{\partial p^{(0)}}{\partial r} = 0, \tag{7.23}$$

$$\frac{\partial p^{(0)}}{\partial x} = \frac{1}{r}\frac{\partial}{\partial r}\left(r\frac{\partial {u_f}^{(0)}}{\partial r}\right), \tag{7.24}$$

under the boundary conditions

$${u_f}^{(0)} = 0 \text{ at } r = h, \frac{\partial {u_f}^{(0)}}{\partial r} = 0 \text{ at } r = 0,\ {v_f}^{(0)} = 0 \text{ at } r = 0, {v_f}^{(0)} = \frac{\partial h}{\partial t} \text{ at } r = h, \tag{7.25}$$

First order:

$$\frac{\partial}{\partial x}[{u_f}^{(1)}] + \frac{1}{r}\frac{\partial}{\partial r}[r{v_f}^{(1)}] = 0, \tag{7.26}$$

$$\frac{\partial p^{(1)}}{\partial r} + \frac{3}{2}C^{(0)}\frac{\partial p^{(0)}}{\partial r} = 0, \tag{7.27}$$

$$Re_0\left(\frac{\partial {u_f}^{(0)}}{\partial t}+{u_f}^{(0)}\frac{\partial {u_f}^{(0)}}{\partial x}+{v_f}^{(0)}\frac{\partial {u_f}^{(0)}}{\partial r}\right)=-\frac{\partial p^{(1)}}{\partial x}-\frac{3}{2}C^{(1)}\frac{\partial p^{(0)}}{\partial x}$$
$$+\frac{3}{2}C^{(1)}\frac{1}{r}\frac{\partial}{\partial r}\left(r\frac{\partial {u_f}^{(0)}}{\partial r}\right)+\frac{1}{r}\frac{\partial}{\partial r}\left(r\frac{\partial {u_f}^{(1)}}{\partial r}\right)\Bigg\}+MC^{(1)}({u_p}^{(0)}-{u_f}^{(0)}), \quad (7.28)$$

$$C^{(1)}\left(\frac{\partial {u_p}^{(0)}}{\partial x}+\frac{1}{r}\left(r\frac{\partial (r{v_p}^{(0)})}{\partial r}\right)\right)=0, \quad (7.29)$$

$$C^{(1)}\frac{\partial p^{(0)}}{\partial r}=0, \quad (7.30)$$

$$C^{(1)}\frac{\partial p^{(0)}}{\partial x}=MC^{(1)}(u_f^{(0)}-u_p^{(0)}), \quad (7.31)$$

under the boundary conditions

$$\begin{aligned}&{u_f}^{(1)}=0 \text{ at } r=h, \frac{\partial {u_f}^{(1)}}{\partial r}=0 \text{ at } r=0,\\ &{v_p}^{(0)}=0 \text{ at } r=h, {v_f}^{(1)}=0 \text{ at } r=0, \ \frac{\partial {u_p}^{(0)}}{\partial r}=0 \text{ at } r=0,\end{aligned} \quad (7.32)$$

Second-order:

$$\frac{\partial}{\partial x}[{u_f}^{(2)}]+\frac{1}{r}\frac{\partial}{\partial r}[r{v_f}^{(2)}]=0, \quad (7.33)$$

$$\frac{\partial p^{(2)}}{\partial r}+\frac{3}{2}C^{(1)}\frac{\partial p^{(1)}}{\partial r}-\frac{5}{2}{C^{(1)}}^2\frac{\partial p^{(0)}}{\partial r}=0, \quad (7.34)$$

$$Re_0\Bigg[\left(\frac{\partial {u_f}^{(1)}}{\partial t}+{u_f}^{(1)}\frac{\partial {u_f}^{(0)}}{\partial x}+{u_f}^{(0)}\frac{\partial {u_f}^{(1)}}{\partial x}+{v_f}^{(1)}\frac{\partial {u_f}^{(0)}}{\partial r}+{v_f}^{(0)}\frac{\partial {u_f}^{(1)}}{\partial r}\right)$$
$$-C^{(1)}\left(\frac{\partial {u_f}^{(0)}}{\partial t}+{u_f}^{(0)}\frac{\partial {u_f}^{(0)}}{\partial x}+{v_f}^{(0)}\frac{\partial {u_f}^{(0)}}{\partial r}\right)\Bigg]=$$
$$-\frac{\partial p^{(2)}}{\partial x}-\frac{3}{2}C^{(1)}\frac{\partial p^{(1)}}{\partial x}+\frac{5}{2}{C^{(1)}}^2\frac{\partial p^{(0)}}{\partial x}+\frac{1}{r}\frac{\partial}{\partial x}\left(r\frac{\partial {u_f}^{(2)}}{\partial r}\right)$$
$$-\frac{5}{2}{C^{(1)}}^2\frac{1}{r}\frac{\partial}{\partial r}\left(r\frac{\partial {u_f}^{(0)}}{\partial r}\right)+\frac{3}{2}C^{(1)}\frac{1}{r}\frac{\partial}{\partial r}\left(r\frac{\partial {u_f}^{(1)}}{\partial r}\right)+MC^{(1)}({u_p}^{(1)}-{u_f}^{(1)}), \quad (7.35)$$

$$C^{(1)}\left(\frac{\partial {u_p}^{(1)}}{\partial x}+\frac{1}{r}\frac{\partial (r{v_p}^{(1)})}{\partial r}\right)=0, \quad (7.36)$$

$$C^{(1)}\frac{\partial p^{(1)}}{\partial r}+\frac{5}{2}{C^{(1)}}^2\frac{\partial p^{(0)}}{\partial r}=0, \quad (7.37)$$

$$\rho Re_0 C^{(1)}\left(\frac{\partial {u_p}^{(0)}}{\partial t}+{u_p}^{(0)}\frac{\partial {u_p}^{(0)}}{\partial x}+{v_p}^{(0)}\frac{\partial {u_p}^{(0)}}{\partial r}\right)=-C^{(1)}\frac{\partial p^{(1)}}{\partial x}$$
$$-\frac{5}{2}{C^{(1)}}^2\frac{\partial p^{(0)}}{\partial x}+MC^{(1)}({u_f}^{(1)}-{u_p}^{(1)}). \quad (7.38)$$

under the boundary conditions

$${u_f}^{(2)}=0 \text{ at } r=h, \frac{\partial {u_f}^{(2)}}{\partial r}=0 \text{ at } r=0, {v_f}^{(2)}=0 \text{ at } r=0,$$
$${v_p}^{(1)}=0 \text{ at } r=0, \frac{\partial {u_p}^{(1)}}{\partial r}=0 \text{ at } r=0, \quad (7.39)$$

We wish to present the analytical consequences in terms of time-averaged volume flow rate which is defined by $\tilde{Q}(x) = \int_0^1 Q(x,t)dt$. The instantaneous volume flow rate $Q(x,t)$ of the suspension in the fixed (R,X) coordinate system is the sum of the instantaneous volume flow rates of the fluid phase, i.e. $Q_f(x,t) = 2\int_0^h (1-C)ru_f dr$, and the particle phase, i.e. $Q_p(x,t) = 2\int_0^h Cru_p dr$, given by

$$Q(x,t) = Q_f(x,t) + Q_p(x,t), \tag{7.40}$$

For the sake of solution, we use transformation from the unsteady laboratory frame to steady wave frame.

The wave frame parameters, given on the left side of the equality sign, are related to the corresponding parameters in the laboratory frame, given on the right side, in the non-dimensional form by

$$X = x - t, R = r, U_i(R,X) = u_i(r,x,t) - 1, V_i(R,X) = v_i(x,r,t), q = Q(x,t) - h^2. \tag{7.41}$$

where $(R,X), (U_i, V_i)$ (with $i = f, p$) and q are in the wave frame.

In view of equation (7.41), $\tilde{Q}(x) = q + \int_0^1 h^2 dt$, and accordingly

$$q = Q(x,t) - h^2 = \tilde{Q}(x) - e^{2bx} + \phi e^{(b+\omega)x} - \frac{3}{8}\phi^2 e^{2\omega x}. \tag{7.42}$$

For Q and $\tilde{Q}$, the regular perturbation expansions are as follows:

$$Q = Q^{(0)} + \delta Q^{(1)} + \delta^2 Q^{(2)} + o(\delta^3),$$
$$\tilde{Q} = \tilde{Q}^{(0)} + \delta \tilde{Q}^{(1)} + \delta^2 \tilde{Q}^{(2)} + o(\delta^3),$$

7.3.1 Solution for the zeroth order system

Integrating equation (7.24) with respect to r, in conjunction with equation (7.23), and applying the first boundary condition of equation (7.25), we get

$$\frac{\partial {u_f}^{(0)}}{\partial r} = \frac{1}{2} r \frac{\partial p^{(0)}}{\partial x},$$

Again integrating with respect to r and using the second boundary condition of equation (7.25), gives

$${u_f}^{(0)} = \frac{1}{4} \frac{\partial p^{(0)}}{\partial x} (r^2 - h^2), \tag{7.43}$$

Under the third boundary condition of equation (7.25), equation (7.22) together with equation (7.43) yields

$$v_f(0) = \frac{r}{16} \left\{ 4h \frac{\partial h}{\partial x} \frac{\partial p^{(0)}}{\partial x} - \frac{\partial^2 p^{(0)}}{\partial x^2} (r^2 - 2h^2) \right\} \tag{7.44}$$

while equation (7.25) together with equation (7.44) under the fourth condition of equation (7.25) gives

$$\frac{\partial h}{\partial t} = \frac{h^3}{16} \frac{\partial^2 p^{(0)}}{\partial x^2} + \frac{h^2}{4} \frac{\partial h}{\partial x} \frac{\partial p^{(0)}}{\partial x},$$

which gives the zeroth-order pressure gradient

$$\frac{\partial p^{(0)}}{\partial x} = \frac{G(t) + 16\int_0^x h(s,t)\frac{\partial h(s,t)}{\partial t}ds}{h^4}, \tag{7.45}$$

where $G(t)$ is an arbitrary function of t.

Therefore the zero-order system axial pressure gradient will be

$$p^{(0)}(x,t) = p^{(0)}(0,t) + \int_0^x \frac{G(t) + 16\int_0^{x_1} h(s,t)\frac{\partial h(s,t)}{\partial t}ds}{h^4(x_1,t)}dx_1. \tag{7.46}$$

The arbitrary function $G(t)$, obtained by putting $x = l$ in equation (7.46), will be

$$G(t) = \frac{\{p^0(l,t) - p^0(0,t)\} - 16\int_0^l \frac{\int_0^{x_1} h(s,t)\frac{\partial h(s,t)}{\partial t}ds}{h^4(x_1,t)}dx_1}{\int_0^l \frac{1}{h^4(x_1,t)}dx_1} \tag{7.47}$$

Further, the flow rate at the zeroth order system, in view of equation (7.40), may be given by

$$Q^{(0)} = {Q_f}^{(0)} + {Q_p}^{(0)} = 2\int_0^h r{u_f}^{(0)}dr + 0 = -\frac{1}{8}\frac{\partial p^{(0)}}{\partial x}h^4.$$

Note that, in an aspect of equation (7.42), we have

$$Q^{(0)} = \tilde{Q}^{(0)} - e^{2bx} + \phi e^{(b+\omega)x} - \frac{3}{8}\phi^2 e^{2\omega x} + h^2.$$

and hence

$$\frac{\partial p^{(0)}}{\partial x} = -8\left\{\frac{\tilde{Q}^{(0)} - e^{2bx} + \phi e^{(b+\omega)x} - \frac{3}{8}\phi^2 e^{2\omega x} + h^2}{h^4}\right\} = P_0 \text{ (Say)} \tag{7.48}$$

Hence, from equations (7.43), (7.44) and (7.48), the axial and radial velocities of the fluid at zero-order system, in terms of time-averaged volume flow rate at zero order system, are given by

$$u_f{}^0 = \frac{1}{4}P_0(r^2 - h^2). \tag{7.49}$$

$$v_f{}^{(0)} = \frac{r}{16}\left\{4hP_0\frac{\partial h}{\partial x} - \frac{\partial P_0}{\partial x}(r^2 - 2h^2)\right\}. \tag{7.50}$$

7.3.2 Solution of the first-order system

So far the zeroth order solution for the fluid part have been deduced. The particulate matter, however, requires relations equations (7.29) and (7.31) obtained for the first order system. Hence, they will be deduced in this section.

The zeroth order axial velocity of the solid particles is deduced by means of equations (7.31) and (7.49) as

$$u_p{}^{(0)} = \frac{1}{4}\left(r^2 - h^2 - \frac{4}{M}\right)P_0. \tag{7.51}$$

Substituting the axial component from equation (7.51) in equation (7.29), the radial velocity of the particulate phase of the zeroth-order system is derived under the first boundary condition of equation (7.32) as

$$v_p{}^{(0)} = \frac{r}{16}\left\{4P_0 h\frac{\partial h}{\partial x} - \frac{\partial P_0}{\partial x}\left(r^2 - 2h^2 - \frac{8}{M}\right)\right\}. \tag{7.52}$$

Equations (7.26)-(7.28) of the first-order system are solved in the similar way to obtain the axial and radial velocities of the fluid of the first-order system given by

$$u_f{}^{(1)} = N_1(r^6 - h^6) + N_2(r^4 - h^4) + \left(N_3 + \frac{P_1 + C^{(1)}P_0}{4}\right)(r^2 - h^2). \tag{7.53}$$

$$\begin{aligned} v_f{}^{(1)} = -\frac{1}{8}\frac{\partial N_1}{\partial x}(r^7 - 4h^6 r) - \frac{1}{6}\frac{\partial N_2}{\partial x}(r^5 - 3rh^4) - \frac{1}{4}\Big(\frac{\partial N_3}{\partial x} \\ + \frac{1}{4}\frac{\partial P_1}{\partial x} + \frac{C^{(1)}}{4}\frac{\partial P_0}{\partial x}\Big)(r^3 - 2rh^2) + \frac{1}{4}(12N_1 + 8N_2h^3 \\ + 2N_3 h + P_1 h + P_0 h C^{(1)})\frac{\partial h}{\partial x}r. \end{aligned} \tag{7.54}$$

The expressions for P_1, N_1, N_2 and N_3 are given by

$$P_1 = \frac{\partial P^{(1)}}{\partial x} = -6N_1h^4 - \frac{16}{3}N_2h^2 - 4N_3 - \frac{P_0}{h^2}C^{(1)}\left(h^2 + \frac{8}{M}\right) - \frac{8\tilde{Q}^{(1)}}{h^4}. \tag{7.55}$$

$$N_1 = \frac{Re_0}{1152}P_0\frac{\partial P_0}{\partial x}. \tag{7.56}$$

$$N_2 = \frac{Re_0}{768}\left(16\frac{\partial P_0}{\partial x} - 3P_0\frac{\partial P_0}{\partial x}h^2\right). \tag{7.57}$$

$$N_3 = Re_0\left(-\frac{h^2}{16}\frac{\partial P_0}{\partial t} - \frac{P_0}{8}\frac{\partial h}{\partial t}h + \frac{P_0}{64}\frac{\partial P_0}{\partial x}h^4 + \frac{{P_0}^2h^3}{32}\frac{\partial h}{\partial x}\right). \tag{7.58}$$

and

$$\tilde{Q}^{(1)} = Q^{(1)} = -\frac{3}{4}N_1h^8 - \frac{2}{3}N_2h^6 - \left(\frac{N_3}{2} + \frac{1}{8}\frac{\partial P^{(1)}}{\partial x} + \frac{P_0}{8}C^{(1)}\right)h^4 - \frac{P_0}{M}C^{(1)}h^2.$$

7.3.3 Solution for the second-order system

In this section too, first of all we will formulate the particulate phase velocity of the first order which requires some of the second order equations. Using the equations ((7.51)-(7.53)) in equation (7.38), the axial velocity of the solid particles of the second-order system is given by

$$\begin{aligned} {u_p}^{(1)} = N_1(r^6 - h^6) + N_2(r^4 - h^4) - \frac{\rho Re_0P_0}{32M}\frac{\partial P_0}{\partial x}(r^4 + h^4) + \Big\{N_3 + \frac{P_1 + C^{(1)}P_0}{4} - \\ \frac{\rho Re_0}{8M}(2\frac{\partial P_0}{\partial t} - \frac{4P_0}{M}\frac{\partial P_0}{\partial x} - {P_0}^2h\frac{\partial h}{\partial x})\Big\}(r^2 - h^2) + \frac{\rho Re_0P_0}{16M}\frac{\partial P_0}{\partial x}r^2h^2 \\ - \frac{\rho Re_0P_0}{8}\Big\{P_0(r^2 + \frac{4}{M})h\frac{\partial h}{\partial x} + \frac{1}{4}\frac{\partial h}{\partial x}(r^2(h^2 + \frac{8}{M}) + \frac{32}{M})\Big\} - \frac{P_1}{M} - \frac{5}{2M}C^{(1)}P_0. \end{aligned} \tag{7.59}$$

Further, equation (7.36), in view of equation (7.59), under the fifth boundary condition equation (7.39), is solved to get the second order radial velocity of the solid particles as

$$
\begin{aligned}
v_p{}^{(1)} = &-\frac{1}{8}\frac{\partial N_1}{\partial x}\left(r^7-4rh^6\right)-\frac{1}{6}\frac{\partial N_2}{\partial x}\left(r^5-3rh^4\right)+3N_1rh^5\frac{\partial h}{\partial x}+2N_2rh^3\frac{\partial h}{\partial x}\\
&+\left(\frac{\rho Re_0P_0}{192M}\frac{\partial^2P_0}{\partial x^2}+\frac{\rho Re_0}{192M}\left(\frac{\partial P_0}{\partial x}\right)^2\right)\left(r^5+3rh^4-3r^3h^2\right)-\left(\frac{\rho Re_0P_0}{192M}\frac{\partial^2P_0}{\partial x^2}\right.\\
&\left.+\frac{\rho Re_0}{192M}\left(\frac{\partial P_0}{\partial x}\right)^2\right)\left(r^3-2rh^2\right)+\left(\frac{P_1}{4}+\frac{\rho Re_0P_0}{2M^2}\frac{\partial P_0}{\partial x}+\frac{\rho Re_0P_0}{2M}\frac{\partial P_0}{\partial x}\right)rh\frac{\partial h}{\partial x}\\
&+\frac{\rho Re_0P_0}{2M}\left(\frac{\partial h}{\partial x}\right)^2r-\frac{\rho Re_0P_0}{32M}\frac{\partial P_0}{\partial x}\frac{\partial h}{\partial x}r^3h-\frac{C^{(1)}}{16}\frac{\partial P_0}{\partial x}r^3-\frac{1}{16}\frac{\partial P_1}{\partial x}r^3+\frac{1}{2M}\frac{\partial P_1}{\partial x}r\\
&+\frac{5C^{(1)}}{4M}\frac{\partial P_0}{\partial r}r+\left(\frac{3\rho Re_0P_0}{16M}\frac{\partial P_0}{\partial x}\frac{\partial h}{\partial x}+\frac{\rho Re_0{P_0}^2}{16M}\frac{\partial^2h}{\partial x^2}\right)rh^3+\left(\frac{\rho Re_0{P_0}^2}{16M}\left(\frac{\partial h}{\partial x}\right)^2\right.\\
&\left.+\frac{1}{8}\frac{\partial P_1}{\partial x}\right)rh^2+\frac{\rho Re_0P_0}{4M}\frac{\partial^2h}{\partial x^2}rh+\left(\frac{\rho Re_0}{16M}\frac{\partial^2P_0}{\partial x^2}+\frac{\rho Re_0P_0}{32}\left(\frac{\partial h}{\partial x}\right)^2-\frac{1}{4}\frac{\partial N_3}{\partial x}\right.\\
&\left.-\frac{\rho Re_0}{16M}\frac{\partial}{\partial x}\left(\frac{\partial P_0}{\partial t}\right)-\frac{\rho Re_0{P_0}^2}{32M}\left(\frac{\partial h}{\partial x}\right)^2\right)r^3+\frac{\rho Re_0}{128}\frac{\partial^2P_0}{\partial x^2}r^3h^2+\left(\frac{\rho Re_0P_0}{16}\frac{\partial P_0}{\partial x}\frac{\partial h}{\partial x}\right.\\
&\left.+\frac{\rho Re_0P_0}{32}\frac{\partial^2h}{\partial x^2}+\frac{\rho Re_0}{64}\frac{\partial P_0}{\partial x}\frac{\partial h}{\partial x}-\frac{\rho Re_0P_0}{16M}\frac{\partial P_0}{\partial x}\frac{\partial h}{\partial x}-\frac{\rho Re_0{P_0}^2}{32M}\frac{\partial^2h}{\partial x^2}\right)r^3h+\left(N_3\frac{\partial h}{\partial x}\right.\\
&\left.+\frac{C^{(1)}P_0}{4}\frac{\partial h}{\partial x}-\frac{\rho Re_0}{8M}\frac{\partial P_0}{\partial t}\frac{\partial h}{\partial x}\right)rh+\left(\frac{\rho Re_0{P_0}^2}{8M}\left(\frac{\partial h}{\partial x}\right)^2\right.\\
&\left.+\frac{1}{2}\frac{\partial N_3}{\partial x}+\frac{C^{(1)}}{8}\frac{\partial P_0}{\partial x}-\frac{\rho Re_0}{8M}\frac{\partial}{\partial x}\left(\frac{\partial P_0}{\partial t}\right)\right)rh^2. \qquad (7.60)
\end{aligned}
$$

The second order axial velocity of the fluid is derived from equation (7.35) by using equations (7.49), (7.53) and (7.59) under the second boundary condition of equation (7.39), as

$$
\begin{aligned}
u_f{}^{(2)} = &\alpha_1\left(r^{10}-h^{10}\right)+\alpha_2\left(r^8-h^8\right)+\alpha_3\left(r^6-h^6\right)+\alpha_4\left(r^4-h^4\right)\\
&+\alpha_5\left(r^2-h^2\right)+\frac{1}{8}\left(2P_2-3C^{(1)}P_1-6{C^{(1)}}^2P_0-12C^{(1)}N_3\right)\left(r^2-h^2\right). \qquad (7.61)
\end{aligned}
$$

And then using equation (7.61) in equation (7.33) under the boundary condition equation (7.39), the second-order radial velocity is given by

$$
\begin{aligned}
{v_f}^{(2)} = &-\frac{1}{12}\frac{\partial \alpha_1}{\partial x}\left(r^{11}-6rh^{10}\right)-\frac{1}{10}\frac{\partial \alpha_2}{\partial x}\left(r^{9}-5rh^{8}\right)-\frac{1}{8}\frac{\partial \alpha_3}{\partial x}\left(r^{7}-4rh^{6}\right)\\
&-\frac{1}{6}\frac{\partial \alpha_4}{\partial x}\left(r^{5}-3rh^{4}\right)-\frac{1}{4}\frac{\partial \alpha_5}{\partial x}\left(r^{3}-2rh^{2}\right)+5\alpha_1 h^9\frac{\partial h}{\partial x}r+4\alpha_2 h^7\frac{\partial h}{\partial x}r\\
&+3\alpha_3 h^5\frac{\partial h}{\partial x}r+2\alpha_4 h^3\frac{\partial h}{\partial x}r+\alpha_5 h\frac{\partial h}{\partial x}r+\frac{1}{32}\Bigg(2\frac{\partial P_2}{\partial x}-3C^{(1)}\frac{\partial P_1}{\partial x}\\
&-6{C^{(1)}}^2\frac{\partial P_0}{\partial x}-12C^{(1)}\frac{\partial N_3}{\partial x}\Bigg)\left(2rh^2-r^3\right)+\Big(2P_2-3C^{(1)}P_1-6{C^{(1)}}^2P_0\\
&-12C^{(1)}N_3\Big)\frac{h}{8}\frac{\partial h}{\partial x}r+\frac{3C^{(1)}}{16}\frac{\partial N_1}{\partial x}\left(r^7-4rh^6\right)+\frac{3C^{(1)}}{12}\frac{\partial N_2}{\partial x}\left(r^5-3rh^4\right)\\
&-\frac{9}{2}N_1C^{(1)}h^5\frac{\partial h}{\partial x}r-3N_2C^{(1)}h^3\frac{\partial h}{\partial x}r. \qquad (7.62)
\end{aligned}
$$

where

$$
\begin{aligned}
P_2 = \frac{\partial p^{(2)}}{\partial x} = &\frac{3}{2}C^{(1)}P_1+3{C^{(1)}}^2P_0+6C^{(1)}N_3-4\alpha_5+\frac{2\rho Re_0}{M}\Bigg(\frac{\partial P_0}{\partial t}-\frac{2P_0}{M}\frac{\partial P_0}{\partial x}\\
&+\frac{2}{M}\frac{\partial P_0}{\partial x}\Bigg)-\frac{8C^{(1)}}{h^2M}\left(P_1+\frac{5}{2}P_0C^{(1)}+\rho Re_0P_0\frac{\partial P_0}{\partial x}\right)+\Bigg\{8C^{(1)}N_2-\frac{16}{3}\alpha_4\\
&+C^{(1)}\left(1-\frac{\rho Re_0P_0}{12M}\right)\frac{\partial P_0}{\partial x}\Bigg\}h^2-6\alpha_3h^4+\left(9C^{(1)}N_1-\frac{32}{5}\alpha_2\right)h^6\\
&-\frac{\rho Re_0{P_0}^2C^{(1)}}{2M}h\frac{\partial h}{\partial x}-10\alpha_1h^8-8\frac{\tilde{Q}^{(2)}}{h^4}. \qquad (7.63)
\end{aligned}
$$

$$
\alpha_1 = Re_0\left(\frac{N_1}{400}\frac{\partial P_0}{\partial x}-\frac{3P_0}{1600}\frac{\partial N_1}{\partial x}\right),
$$

$$\alpha_2 = Re_0\left\{\frac{P_0N_1}{64}\frac{\partial h}{\partial x}h-\left(\frac{N_1}{256}\frac{\partial P_0}{\partial x}+\frac{P_0}{256}\frac{\partial N_1}{\partial x}\right)h^2+\frac{N_2}{256}\frac{\partial P_0}{\partial x}+\frac{2P_0}{768}\frac{\partial N_2}{\partial x}\right\},$$

$$\begin{aligned}\alpha_3 = Re_0\Bigg\{&\frac{P_0N_2h}{72}\frac{\partial h}{\partial x}-\frac{N_2h^2}{144}\frac{\partial P_0}{\partial x}+\frac{N_3}{36}+\frac{P_1+C^{(1)}P_0}{72}\\&+\frac{P_0}{288}\left(\frac{\partial N_3}{\partial x}+\frac{3}{4}\frac{\partial P_1}{\partial x}+\frac{3C^{(1)}}{4}\frac{\partial P_0}{\partial x}\right)-\frac{P_0h^2}{144}\frac{\partial N_2}{\partial x}+\frac{C^{(1)}P_0}{5760}\frac{\partial P_0}{\partial x}\\&+\frac{C^{(1)}\rho P_0}{1152}\frac{\partial P_0}{\partial x}\Bigg\},\end{aligned}$$

$$\begin{aligned}\alpha_4 = Re_0\Bigg\{&\frac{1}{64}\frac{\partial P_0}{\partial t}-\frac{N_1h^6}{64}\frac{\partial P_0}{\partial x}-\frac{N_2h^4}{64}\frac{\partial P_0}{\partial x}-\frac{h^2}{8}\Bigg(N_3\\&+\frac{P_1+C^{(1)}P_0}{2}\Bigg)-\frac{P_0h^2}{64}\left(\frac{\partial N_3}{\partial x}+\frac{3}{4}\frac{\partial P_1}{\partial x}+\frac{3C^{(1)}}{4}\frac{\partial P_0}{\partial x}\right)\\&+\frac{P_0}{128}\frac{\partial h}{\partial x}\Big(12N_1+8N_2h^3+2N_3h+P_1h+P_0hC^{(1)}\Big)\\&-\frac{P_0h^6}{64}\frac{\partial N_1}{\partial x}-\frac{3P_0N_1h^5}{32}\frac{\partial h}{\partial x}-\frac{P_0h^3N_2}{16}\frac{\partial h}{\partial x}\Bigg\},\end{aligned}$$

$$\alpha_5 = Re_0\Big\{-\frac{h^2}{16}\frac{\partial P_0}{\partial t}-\frac{P_0 h}{8}\frac{\partial h}{\partial t}+\frac{N_1 h^8}{16}\frac{\partial P_0}{\partial x}+\frac{N_2 h^6}{16}\frac{\partial P_0}{\partial x}$$
$$+\frac{h^4}{4}\left(N_3+\frac{P_1+C^{(1)}P_0}{2}\right)+\frac{N_1 P_0 h^7}{2}\frac{\partial h}{\partial x}+\frac{3N_2 P_0 h^5}{8}\frac{\partial h}{\partial x}+\frac{P_0 h^8}{16}$$
$$\frac{\partial N_1}{\partial x}+\frac{P_0 h^6}{16}\frac{\partial N_2}{\partial x}+\frac{P_0 h^4}{16}\left(\frac{\partial N_3}{\partial x}+\frac{1}{2}\frac{\partial P_1}{\partial x}+\frac{C^{(1)}}{2}\frac{\partial P_0}{\partial x}\right)+\frac{C^{(1)}h^2}{16}\frac{\partial P_0}{\partial t}$$
$$+\frac{C^{(1)}P_0 h}{8}\frac{\partial h}{\partial t}+\frac{P_0 h^4}{64}\frac{\partial P_0}{\partial x}-\frac{{P_0}^2 h^3}{32}\frac{\partial h}{\partial x}-\frac{C^{(1)}\rho h^2}{32}\Big(2\frac{\partial P_0}{\partial t}-\frac{4P_0}{M}\frac{\partial P_0}{\partial x}$$
$$-{P_0}^2 h\frac{\partial h}{\partial x}\Big)-\frac{C^{(1)}\rho {P_0} h^4}{128}\frac{\partial P_0}{\partial x}+\frac{2C^{(1)}P_1+5{C^{(1)}}^3 P_0}{4}+\frac{\rho {P_0}^2 h}{8}\frac{\partial h}{\partial x}+2C^{(1)}\frac{\partial P_0}{\partial x}\Big\}.$$

and

$$\tilde{Q}^{(2)} = Q^{(2)} = \frac{h^4}{8}\Big[\frac{3}{2}C^{(1)}P_1+3{C^{(1)}}^2 P_0+6C^{(1)}N_3-4\alpha_5+\frac{2\rho Re_0}{M}\Big(\frac{\partial P_0}{\partial t}$$
$$-\frac{2P_0}{M}\frac{\partial P_0}{\partial x}+\frac{2}{M}\frac{\partial P_0}{\partial x}\Big)\Big]-\frac{C^{(1)}}{M}\left(P_1+\frac{5}{2}P_0 C^{(1)}+\rho Re_0 P_0\frac{\partial P_0}{\partial x}\right)h^2$$
$$+\left\{C^{(1)}N_2-\frac{2}{3}\alpha_4+\frac{C^{(1)}}{8}\left(1-\frac{\rho Re_0 P_0}{12M}\right)\frac{\partial P_0}{\partial x}\right\}h^6-\frac{3}{4}\alpha_3 h^8+\Big(\frac{9}{8}C^{(1)}N_1$$
$$-\frac{4}{5}\alpha_2\Big)h^{10}-\frac{\rho Re_0 {P_0}^2 C^{(1)}}{16M}\frac{\partial h}{\partial x}h^5-\frac{5}{4}\alpha_1 h^{12}-\frac{P_2}{8}h^4. \quad (7.64)$$

The solutions given in equations (7.17)-(7.21) together constitute the required results for the fluid and particulate velocities, and the pressure gradient in terms of time-averaged volume flow rate. Therefore, the axial and radial velocities of the fluid in the fixed frame, and the pressure gradient are as follows:

$$u_f = \frac{P_0}{4}\left(r^2 - h^2\right) + \delta\Big\{N_1\left(r^6 - h^6\right) + N_2\left(r^4 - h^4\right) + \left(N_3 + \frac{P_1 + C^{(1)}P_0}{4}\right)$$
$$\left(r^2 - h^2\right)\Big\} + \delta^2\Big\{\alpha_1\left(r^{10} - h^{10}\right) + \alpha_2\left(r^8 - h^8\right) + \alpha_3\left(r^6 - h^6\right) + \alpha_4\left(r^4 - h^4\right) + \alpha_5$$
$$\left(r^2 - h^2\right) + \left(\frac{2P_2 - 3C^{(1)}P_1 - 6{C^{(1)}}^2P_0 - 12C^{(1)}N_3}{8}\right)\left(r^2 - h^2\right)\Big\}. \quad (7.65)$$

$$v_f = \frac{r}{4}\Big\{h\frac{\partial h}{\partial x}P_0 - \frac{\partial P_0}{\partial x}\left(\frac{r^2}{4} - \frac{h^2}{2}\right)\Big\} + \delta\Big\{-\frac{1}{8}\frac{\partial N_1}{\partial x}\left(r^7 - 4h^6r\right) - \frac{1}{6}\frac{\partial N_2}{\partial x}\Big(r^5$$
$$- 3rh^4\Big) - \frac{1}{4}\left(\frac{\partial N_3}{\partial x} + \frac{1}{4}\frac{\partial P_1}{\partial x} + \frac{C^{(1)}}{4}\frac{\partial P_0}{\partial x}\right)\left(r^3 - 2rh^2\right) + \frac{1}{4}\Big(12N_1 + 8N_2h^3$$
$$+ 2N_3h + P_1h + P_0hC^{(1)}\Big)\frac{\partial h}{\partial x}r\Big\} + \delta^2\Big\{-\frac{1}{12}\frac{\partial \alpha_1}{\partial x}\left(r^{11} - 6rh^{10}\right) - \frac{1}{10}\frac{\partial \alpha_2}{\partial x}\Big(r^9$$
$$- 5rh^8\Big) - \frac{1}{8}\frac{\partial \alpha_3}{\partial x}\left(r^7 - 4rh^6\right) - \frac{1}{6}\frac{\partial \alpha_4}{\partial x}\left(r^5 - 3rh^4\right) - \frac{1}{4}\frac{\partial \alpha_5}{\partial x}\left(r^3 - 2rh^2\right)$$
$$+ 5\alpha_1h^9\frac{\partial h}{\partial x}r + 4\alpha_2h^7\frac{\partial h}{\partial x}r + 3\alpha_3h^5\frac{\partial h}{\partial x}r + 2\alpha_4h^3\frac{\partial h}{\partial x}r + \alpha_5h\frac{\partial h}{\partial x}r + \frac{1}{32}\Big(2\frac{\partial P_2}{\partial x}$$
$$- 3C^{(1)}\frac{\partial P_1}{\partial x} - 6{C^{(1)}}^2\frac{\partial P_0}{\partial x} - 12C^{(1)}\frac{\partial N_3}{\partial x}\Big)\Big(2rh^2 - r^3\Big) + \Big(2P_2 - 3C^{(1)}P_1$$
$$- 6{C^{(1)}}^2P_0 - 12C^{(1)}N_3\Big)\frac{h}{8}\frac{\partial h}{\partial x}r + \frac{3C^{(1)}}{16}\frac{\partial N_1}{\partial x}\left(r^7 - 4rh^6\right) + \frac{3C^{(1)}}{12}\frac{\partial N_2}{\partial x}\Big(r^5$$
$$- 3rh^4\Big) - \frac{9}{2}N_1C^{(1)}h^5\frac{\partial h}{\partial x}r - 3N_2C^{(1)}h^3\frac{\partial h}{\partial x}r\Big\}. \quad (7.66)$$

$$u_p = \frac{1}{4}\left(r^2 - h^2 - \frac{4}{M}\right)P_0 + \delta\Big[N_1\left(r^6 - h^6\right) + N_2\left(r^4 - h^4\right) - \frac{\rho Re_0 P_0}{32M}\frac{\partial P_0}{\partial x}$$
$$\left(r^4 + h^4\right) + \left\{N_3 + \frac{P_1 + C^{(1)}P_0}{4} - \frac{\rho Re_0}{8M}\left(2\frac{\partial P_0}{\partial t} - \frac{4P_0}{M}\frac{\partial P_0}{\partial x} - P_0^2 h\frac{\partial h}{\partial x}\right)\right\}\left(r^2\right.$$
$$\left. - h^2\right) + \frac{\rho Re_0 P_0}{16M}\frac{\partial P_0}{\partial x}r^2h^2 - \frac{\rho Re_0 P_0}{8}\left\{P_0 h\left(r^2 + \frac{4}{M}\right)\frac{\partial h}{\partial x} + \frac{1}{4}\frac{\partial P_0}{\partial x}\left(r^2\left(h^2\right.\right.\right.$$
$$\left.\left.\left. + \frac{8}{M}\right) + \frac{32}{M}\right)\right\} - \frac{P_1}{M} - \frac{5}{2M}C^{(1)}P_0\Big]. \quad (7.67)$$

$$v_p = \frac{r}{16}\left\{4P_0 h\frac{\partial h}{\partial x} - \frac{\partial P_0}{\partial x}\left(r^2 - 2h^2 - \frac{8}{M}\right)\right\} + \delta\Big\{-\frac{1}{8}\frac{\partial N_1}{\partial x}\left(r^7 - 4rh^6\right)$$
$$-\frac{1}{6}\frac{\partial N_2}{\partial x}\left(r^5 - 3rh^4\right) + 3N_1 rh^5\frac{\partial h}{\partial x} + 2N_2 rh^3\frac{\partial h}{\partial x} + \left(\frac{\rho Re_0 P_0}{192M}\frac{\partial^2 P_0}{\partial x^2} + \frac{\rho Re_0}{192M}\left(\frac{\partial P_0}{\partial x}\right)^2\right)$$
$$\left(r^5 + 3rh^4 - 3r^3h^2\right) - \left(\frac{\rho Re_0 P_0}{192M}\frac{\partial^2 P_0}{\partial x^2} + \frac{\rho Re_0}{192M}\left(\frac{\partial P_0}{\partial x}\right)^2\right)\left(r^3 - 2rh^2\right) + \left(\frac{P_1}{4}\right.$$
$$\left. + \frac{\rho Re_0 P_0}{2M^2}\frac{\partial P_0}{\partial x} + \frac{\rho Re_0 P_0}{2M}\frac{\partial P_0}{\partial x}\right)rh\frac{\partial h}{\partial x} + \frac{\rho Re_0 P_0}{2M}\left(\frac{\partial h}{\partial x}\right)^2 r - \frac{\rho Re_0 P_0}{32M}\frac{\partial P_0}{\partial x}\frac{\partial h}{\partial x}r^3h$$
$$-\frac{C^{(1)}}{16}\frac{\partial P_0}{\partial x}r^3 - \frac{1}{16}\frac{\partial P_1}{\partial x}r^3 + \frac{1}{2M}\frac{\partial P_1}{\partial x}r + \frac{5C^{(1)}}{4M}\frac{\partial P_0}{\partial r}r + \left(\frac{3\rho Re_0 P_0}{16M}\frac{\partial P_0}{\partial x}\frac{\partial h}{\partial x}\right.$$
$$\left. + \frac{\rho Re_0 {P_0}^2}{16M}\frac{\partial^2 h}{\partial x^2}\right)rh^3 + \left(\frac{\rho Re_0 {P_0}^2}{16M}\left(\frac{\partial h}{\partial x}\right)^2 + \frac{1}{8}\frac{\partial P_1}{\partial x}\right)rh^2 + \frac{\rho Re_0 P_0}{4M}\frac{\partial^2 h}{\partial x^2}rh +$$
$$\left(\frac{\rho Re_0}{16M}\frac{\partial^2 P_0}{\partial x^2} + \frac{\rho Re_0 P_0}{32}\left(\frac{\partial h}{\partial x}\right)^2 - \frac{1}{4}\frac{\partial N_3}{\partial x} - \frac{\rho Re_0}{16M}\frac{\partial}{\partial x}\left(\frac{\partial P_0}{\partial t}\right)\right.$$
$$\left. - \frac{\rho Re_0 {P_0}^2}{32M}\left(\frac{\partial h}{\partial x}\right)^2\right)r^3 + \frac{\rho Re_0}{128}\frac{\partial^2 P_0}{\partial x^2}r^3h^2 + \left(\frac{\rho Re_0 P_0}{16}\frac{\partial P_0}{\partial x}\frac{\partial h}{\partial x} + \frac{\rho Re_0 P_0}{32}\frac{\partial^2 h}{\partial x^2}\right.$$
$$\left. + \frac{\rho Re_0}{64}\frac{\partial P_0}{\partial x}\frac{\partial h}{\partial x} - \frac{\rho Re_0 P_0}{16M}\frac{\partial P_0}{\partial x}\frac{\partial h}{\partial x} - \frac{\rho Re_0 {P_0}^2}{32M}\frac{\partial^2 h}{\partial x^2}\right)r^3h + \left(N_3\frac{\partial h}{\partial x} + \frac{C^{(1)}P_0}{4}\frac{\partial h}{\partial x}\right.$$
$$\left. - \frac{\rho Re_0}{8M}\frac{\partial P_0}{\partial t}\frac{\partial h}{\partial x}\right)rh + \left(\frac{\rho Re_0 {P_0}^2}{8M}\left(\frac{\partial h}{\partial x}\right)^2 + \frac{1}{2}\frac{\partial N_3}{\partial x} + \frac{C^{(1)}}{8}\frac{\partial P_0}{\partial x} - \frac{\rho Re_0}{8M}\frac{\partial}{\partial x}\left(\frac{\partial P_0}{\partial t}\right)\right)rh^2\Big\}.$$

(7.68)

$$p = -8\left(\frac{\tilde{Q}^{(0)} - e^{2bx} + \phi\ e^{(b+\omega)x} - \frac{3}{8}\phi^2 e^{2\omega x} + h^2}{h^4}\right) - \delta\left\{6N_1h^4 + \frac{16}{3}N_2h^2 + 4N_3 - 8C^{(1)}\left(\frac{\tilde{Q}^{(0)} - e^{2bx} + \phi\ e^{(b+\omega)x} - \frac{3}{8}\phi^2 e^{2\omega x} + h^2}{h^6}\right)\left(\frac{8}{M} + h^2\right) + \frac{8\tilde{Q}^{(1)}}{h^4}\right\} + \delta^2\left\{\frac{3}{2}C^{(1)}P_1 + 3C^{(1)^2}P_0 + 6C^{(1)}N_3 - 4\alpha_5 + \frac{2\rho Re_0}{M}\left(\frac{\partial P_0}{\partial t} - \frac{2P_0}{M}\frac{\partial P_0}{\partial x} + \frac{2}{M}\frac{\partial P_0}{\partial x}\right) - \frac{8C^{(1)}}{h^2M}\left(P_1 + \frac{5}{2}P_0C^{(1)} + \rho Re_0P_0\frac{\partial P_0}{\partial x}\right) + \left\{8C^{(1)}N_2 - \frac{16}{3}\alpha_4 + C^{(1)}\left(1 - \frac{\rho Re_0P_0}{12M}\right)\frac{\partial P_0}{\partial x}\right\}h^2 - 6\alpha_3h^4 + \left(9C^{(1)}N_1 - \frac{32}{5}\alpha_2\right)h^6 - \frac{\rho Re_0{P_0}^2C^{(1)}}{2M}h\frac{\partial h}{\partial x} - 10\alpha_1h^8 - 8\frac{\tilde{Q}^{(2)}}{h^4}\right\}. \tag{7.69}$$

For wave number, $\delta \to 0$, equations (7.65)-(7.69) reduce to the corresponding equations derived by Shapiro *et al.* (1969).

7.4 Results and discussion

In order to emphasize the application of the analytical work presented above, in our model consider the motion of a single food bolus through oesophagus suffering from hiatus hernia. The diameter and the length of a normal oesophagus is respectively 1.8-2.1 cm (Joohee *et al.* (2012)) and 25-30 cm (Lamb *et al.* (2005)). Suspended particles are assumed to have a uniform radius 0.04 centimeter. We further assume that the oesophagus can accommodate three boluses at a time while swallowing.

The analytical solutions look appropriate in the fixed frame up to the second order of the time-averaged volume flow rate $\tilde{Q} = \tilde{Q}^0 + \delta\tilde{Q}^1 + \delta^2\tilde{Q}^{(2)}$. Computer codes for the scientific assessment of the analytical results were developed

by using $\tilde{Q}^{(0)} = \tilde{Q} - \delta\tilde{Q}^1 - \delta^2\tilde{Q}^{(2)}$ in the equations (7.65)-(7.69). Plots are drawn for axial, radial velocities as shown in the Figures 7.2-7.15.

7.4.1 Analysis of flow in the relaxed and contracted regions

Figure 7.2 based on the equations (7.59) and (7.65) presents the axial velocities of fluid and solid particles along the axis of the oesophagus at the radial coordinate $r = 0.30$ at time $t = 0.00, 0.40, 0.80$. Other parameters are set as $b = 0.00$, $\omega = 0.00$, $\phi = 0.76$, $\delta = 0.05$, $C^{(1)} = 8.00$, $Re_0 = 8$, $\tilde{Q} = 1.60$, $\tilde{Q}^{(1)} = 18$, $\tilde{Q}^{(2)} = 18$, $M = 2500$.

In Figure 7.2, we observe that wherever the tube is relaxed, the velocities for the fluid and particle phases are positive but negative in the contracted region. At macro level, the fluid is observed to flow faster than the suspended particles throughout its journey in the tube. For different time instants, at each contracted portion of the oesophagus, peaks, indicating the maxima, of the axial velocity of the fluid are almost equal during the transportation of the bolus in the tube. We observe similar patterns also for suspended solid particles. It means that the bolus experiences equal pressure at each contracted portion of the oesophagus at different instants.

7.4.2 Impact of the gradient parameter on flow

We examine the impact of the gradient parameter on the axial velocities of the fluid and the suspended particles in Figures 7.3-7.5. The diagrams display the axial velocities of the fluid and solid particles along the axis of the oesophagus

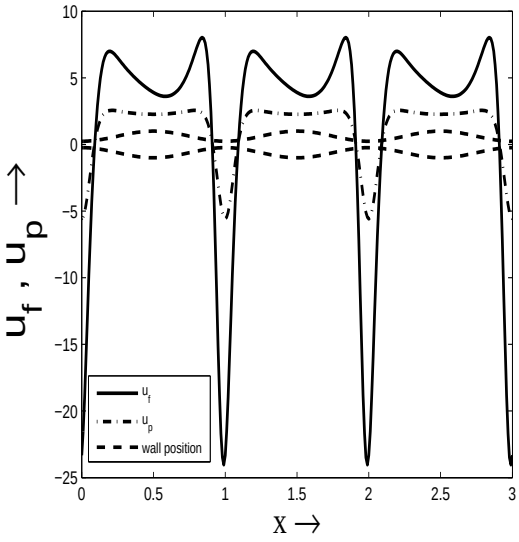

(7.2a) $t = 0.00$

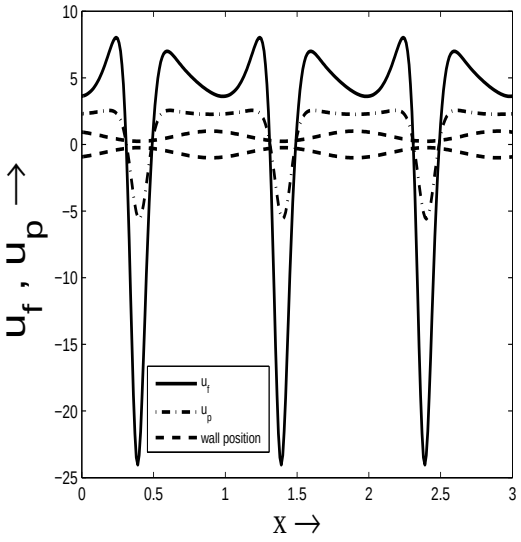

(7.2b) $t = 0.40$

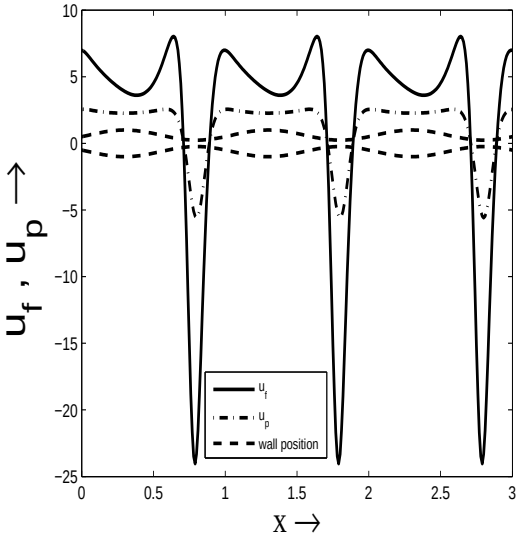

(7.2c) $t = 0.80$

Figure 7.2: Axial velocity profile of the fluid and solid particles versus the tube length at the fixed radial distance $r = 0.30$ and (7.2a) $t = 0.00$ (7.2b) $t = 0.40$ (7.2c) $t = 0.80$. Other parameters are taken as $b = 0.00$, $\omega = 0.00$, $\phi = 0.76$, $\delta = 0.05$, $C^{(1)} = 8.00$, $Re_0 = 8$, $\tilde{Q} = 1.60$, $\tilde{Q}^{(1)} = 18$, $\tilde{Q}^{(2)} = 18$, $M = 2500$.

at the radial length $r = 0.30$ for the instants $t = 0.00, 0.40, 0.80$. Other parameters are set as $\omega = 0.025$, $\phi = 0.76$, $\delta = 0.05$, $C^{(1)} = 8.00$, $Re_0 = 8$, $\tilde{Q} = 1.60$, $\tilde{Q}^{(1)} = 18$, $\tilde{Q}^{(2)} = 18$, $M = 2500$ and $b = 0.00$, $b = 0.04$, $b = 0.08$.

Figures 7.3-7.5 are meant for the comparative study of the impact of the gradient parameter on the flow dynamics under the wave amplitude dilation. Initially (Figure 7.3) the tube is considered uniform (i.e., $b = 0$) with $\omega = 0.025$. The rest of the parameters are fixed as considered for Figure 7.2. As the bolus progresses in the oesophagus, flow reversal in the contracted parts lessens in magnitude. But in the relaxed part, the velocities seem to remain either unchanged or the differences are insignificant. The differences, if any, of the velocities in the relaxed parts are not significant.

We further assign new values 0.04 and 0.08 to b keeping all other parameters constant. Observation is that the flow reversal further diminishes in magnitude and finally disappears (Figures 7.4 and 7.5). Thus we conclude that any divergence in the tube opposes flow reversal even in the contracted regions during the flow. This will eventually increase the flow rate in the oesophagus. This is the case similar to sliding hiatus hernia near the cardiac sphincter.

7.4.3 Effect of the wave-amplitude dilation on flow

Figures (7.6c)-(7.8c) exhibit the axial velocities of the fluid and the particulate suspension at the radial distance $r = 0.30$ at times $t = 0.00, 0.40, 0.80$. Parameters, other than ω, are the same as considered before. The wave amplitude dilation parameter ω is varied in the range 0.00 - 0.04. In Figures (7.6c)-(7.8c), we examine the impact of variation of the dilation parameter on the axial velocities of the fluid and the suspended particles.

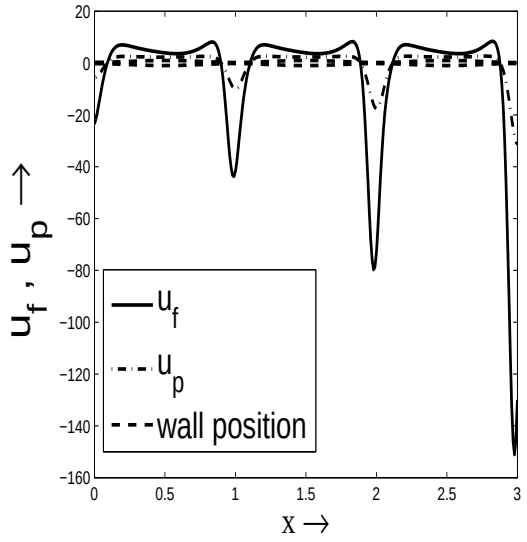

(7.3a) $t = 0.00$

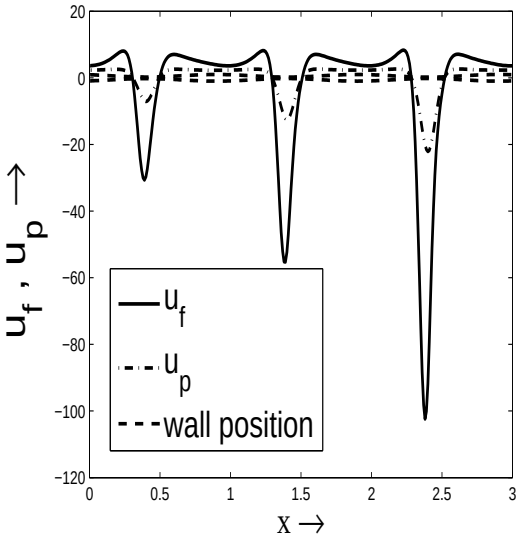

(7.3b) $t = 0.40$

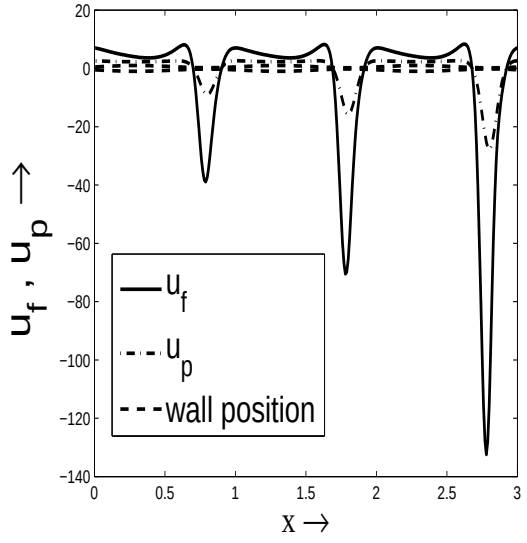

(7.3c) $t = 0.40$

Figure 7.3: Axial velocity profile of the fluid and solid particles versus the tube length at the fixed radial distance $r = 0.30$ and (7.3a) $t = 0.00$ (7.3b) $t = 0.40$ (7.3c) $t = 0.80$. Other parameters are taken as $b = 0.00$, $\omega = 0.025$, $\phi = 0.76$, $\delta = 0.05$, $C^{(1)} = 8.00$, $Re_0 = 8$, $\tilde{Q} = 1.60$, $\tilde{Q}^{(1)} = 18$, $\tilde{Q}^{(2)} = 18$, $M = 2500$.

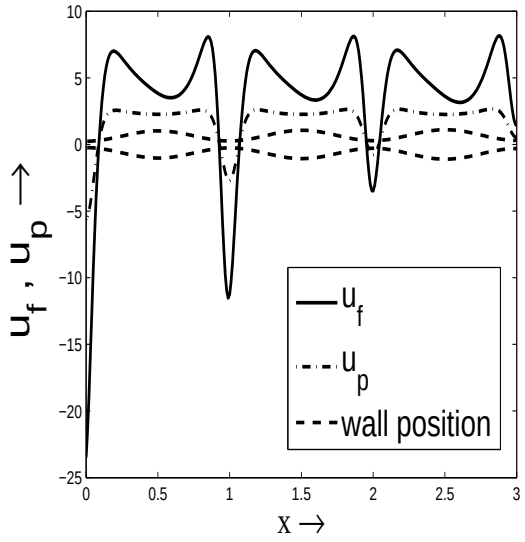

(7.4a) $t = 0.00$

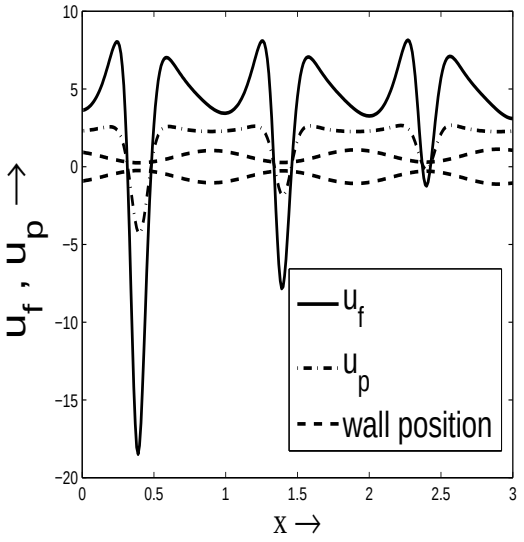

(7.4b) $t = 0.40$

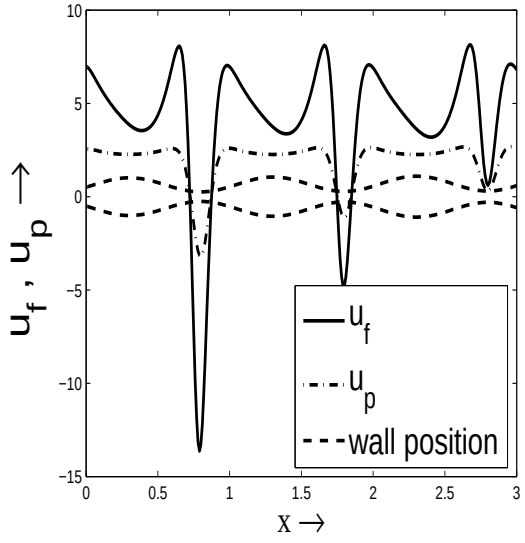

(7.4c) $t = 0.40$

Figure 7.4: Axial velocity profile of the fluid and solid particles versus the tube length at the fixed radial distance $r = 0.30$ and (7.4a) $t = 0.00$ (7.4b) $t = 0.40$ (7.4c) $t = 0.80$. Other parameters are taken as $b = 0.04$, $\omega = 0.025$, $\phi = 0.76$, $\delta = 0.05$, $C^{(1)} = 8.00$, $Re_0 = 8.00$, $\tilde{Q} = 1.60$, $\tilde{Q}^{(1)} = 18$, $\tilde{Q}^{(2)} = 18$, $M = 2500$.

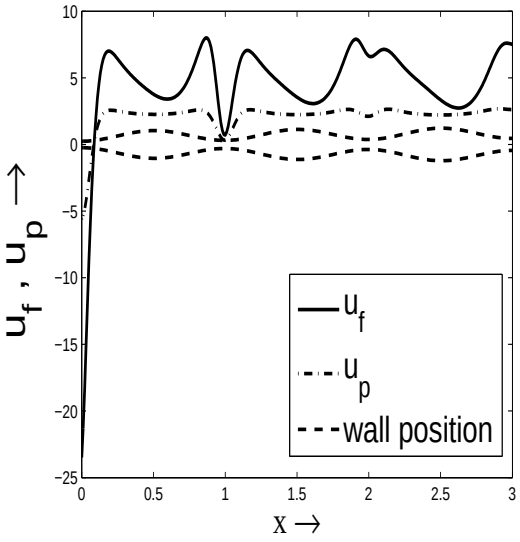

(7.5a) $t = 0.00$

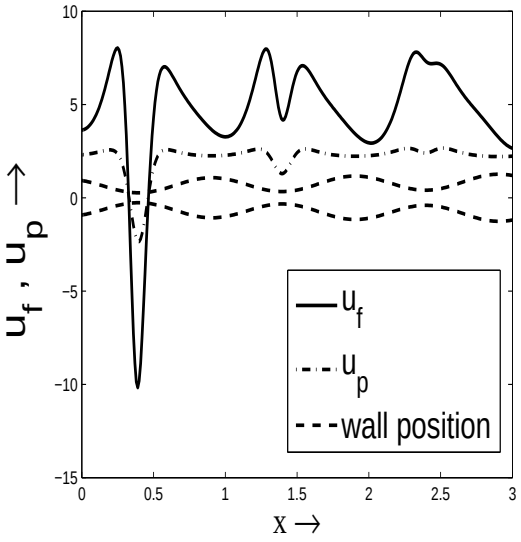

(7.5b) $t = 0.40$

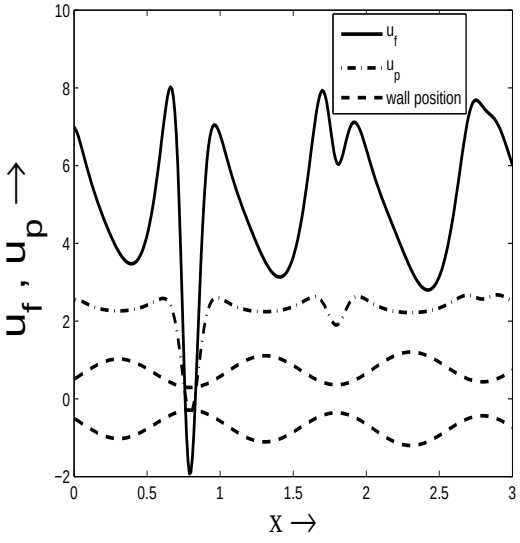

(7.5c) $t = 0.80$

Figure 7.5: Axial velocity profile of the fluid and solid particles versus the tube length at the fixed radial distance $r = 0.30$ and (7.5a) $t = 0.00$ (7.5b) $t = 0.40$ (7.5c) $t = 0.80$. Other parameters are taken as $b = 0.08$, $\omega = 0.025$, $\phi = 0.76$, $\delta = 0.05$, $C^{(1)} = 8.00$, $Re_0 = 8$, $\tilde{Q} = 1.60$, $\tilde{Q}^{(1)} = 18$, $\tilde{Q}^{(2)} = 18$, $M = 2500$.

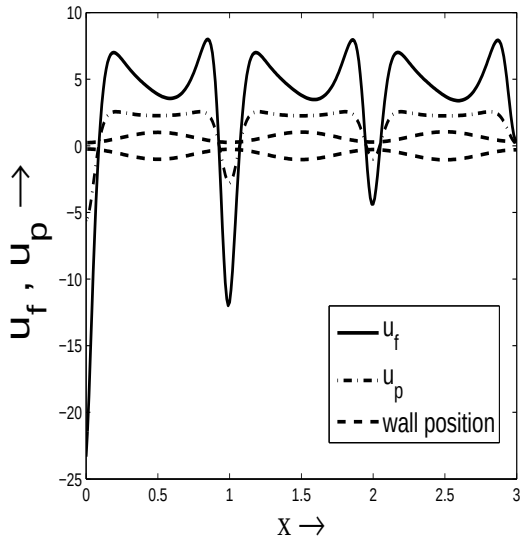

(7.6a) $t = 0.00$

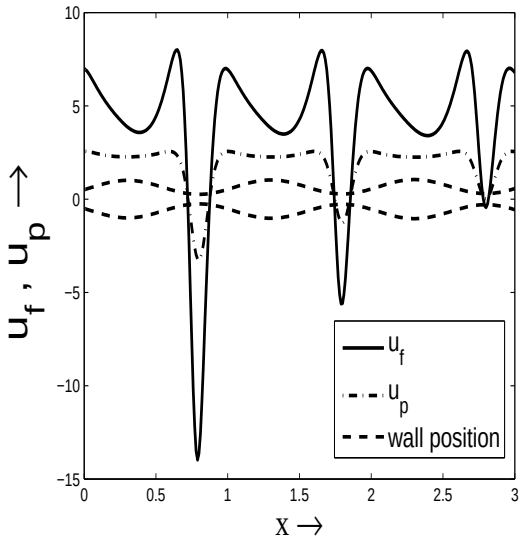

(7.6b) $t = 0.40$

Since the tube diverges, its impact is reflected in terms of diminishing flow reversal in the contracted parts of the tube in Figure (7.6c) in which $\omega = 0$. The impact of ω is reflected in Figures (7.7c) and (7.8c). This is observed that, as expected, it further enhances the flow rate which rises with more dilation of ω (Figures (7.6c)-(7.8c)). This makes swallowing easier in the oesophagus. This is the case similar to sliding hiatus hernia near the cardiac sphincter. This also makes swallowing easier in the oesophagus. Quantitatively, no change is noticed in flow patterns of the fluid and solid velocities.

However, rising dilation of the wave amplitude enhances the flow rate. However unlike gradient parameter, flow reversal in the contracted parts magnifies. Figures (7.7c) and (7.8c) exhibit it very clearly. Here too, no alteration in the two velocity patterns is observed.

Figure (7.9c), based on equations (7.65) and (7.67), presents the radial profile of the axial velocity of the fluid with suspended particles along the axis of the oesophagus at an arbitrarily chosen axial position $x = 0.651$, for the different

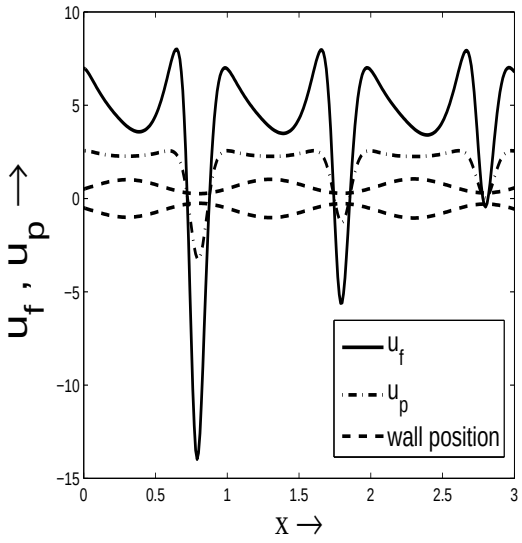

(7.6c) $t = 0.80$

Figure 7.6: Axial velocity profile of the fluid and solid particles versus the tube length at the fixed radial distance $r = 0.30$ and (7.6a) $t = 0.00$ (7.6b) $t = 0.40$ (7.6c) $t = 0.80$. Other parameters are taken as $b = 0.08$, $\omega = 0.025$, $\phi = 0.76$, $\delta = 0.05$, $C^{(1)} = 8.00$, $Re_0 = 8$, $\tilde{Q} = 1.60$, $\tilde{Q}^{(1)} = 18$, $\tilde{Q}^{(2)} = 18$, $M = 2500$.

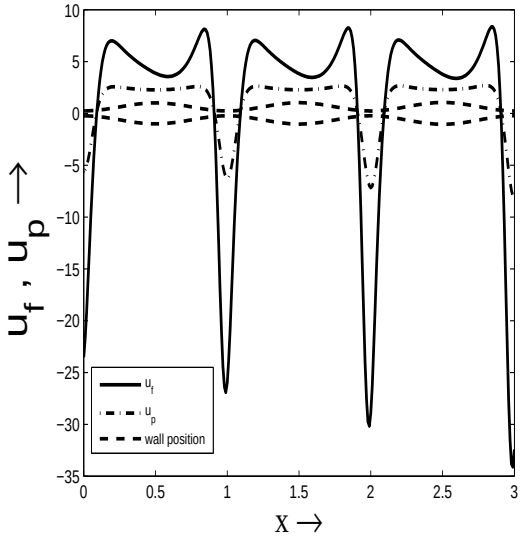

(7.7a) $t = 0.00$

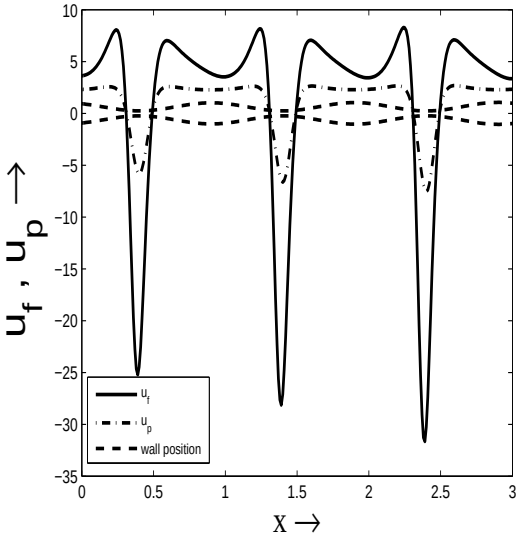

(7.7b) $t = 0.40$

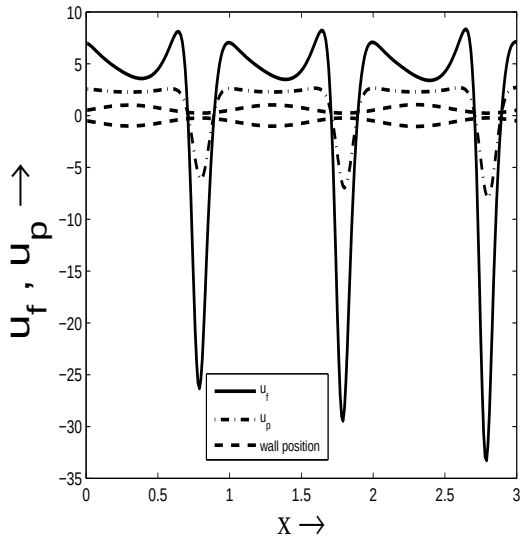

(7.7c) $t = 0.80$

Figure 7.7: Axial velocity profile of the fluid and solid particles versus the tube length at the fixed radial distance $r = 0.30$ and (7.7a) $t = 0.00$ (7.7b) $t = 0.40$ (7.7c) $t = 0.80$. Other parameters are taken as $b = 0.02$, $\omega = 0.003$, $\phi = 0.76$, $\delta = 0.05$, $C^{(1)} = 8.00$, $Re_0 = 8$, $\tilde{Q} = 1.60$, $\tilde{Q}^{(1)} = 18$, $\tilde{Q}^{(2)} = 18$, $M = 2500$.

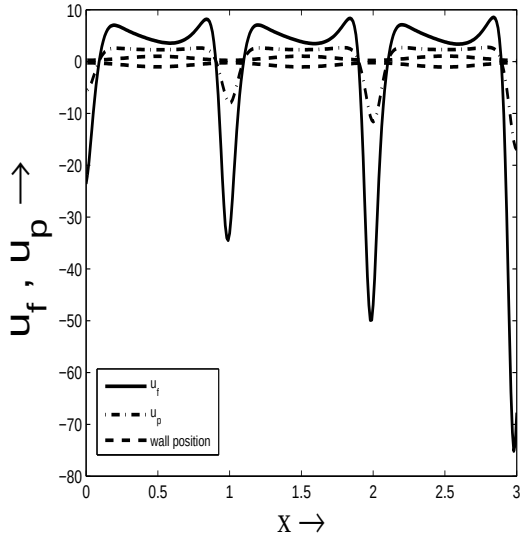

(7.8a) $t = 0.00$

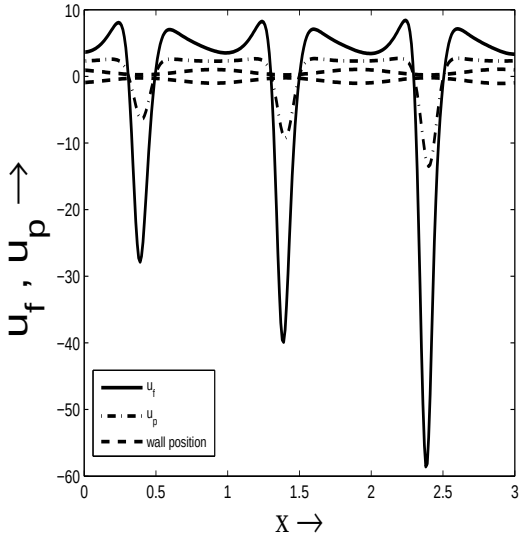

(7.8b) $t = 0.40$

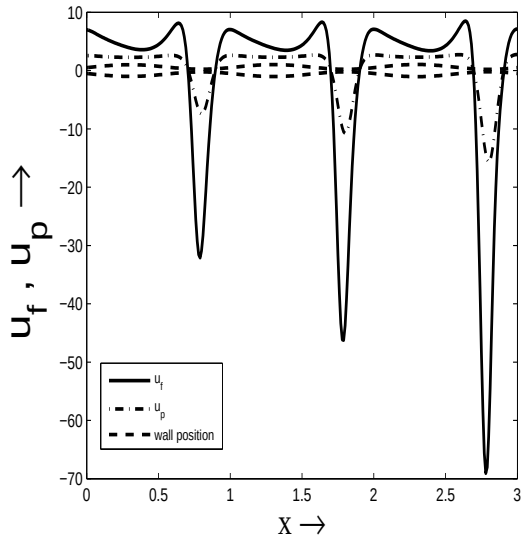

(7.8c) $t = 0.80$

Figure 7.8: Axial velocity profile of the fluid and solid particles versus the tube length at the fixed radial distance $r = 0.30$ and (7.8a) $t = 0.00$ (7.8b) $t = 0.40$ (7.8c) $t = 0.80$. Other parameters are taken as $b = 0.02$, $\omega = 0.04$, $\phi = 0.76$, $\delta = 0.05$, $C^{(1)} = 8.00$, $Re_0 = 8$, $\tilde{Q} = 1.60$, $\tilde{Q}^{(1)} = 18$, $\tilde{Q}^{(2)} = 18$, $M = 2500$.

instants of time $t = 0.00, 0.40, 0.80$. Other parameters are set as $b = 0.004$, $\omega = 0.002$, $\phi = 0.60$, $\delta = 0.05$, $C^{(1)} = 4$, $Re_0 = 8$, $\tilde{Q} = 1.40$, $\tilde{Q}^{(1)} = 18$, $\tilde{Q}^{(2)} = 18$, $M = 1200$. As we observed in Figures 7.2 - 7.8, the fluid moves axially faster than the suspended particles.

The entire discussion so far was limited to the radial profiles of the axial velocities of the fluid and the suspended particulate matter at a fixed radial coordinate $r = 0.3$. This however does not reflect the influence of the condition imposed that while fluid does not slip at the tube boundary, the particulate matter is free to move. To this end, we plot diagrams of the axial fluid and particle velocities along the radius, shown in Figure (7.9c), for arbitrarily selected time instants in a diverging tube under dilating peristaltic waves. The observation is that the axial velocities of the fluid and the particulate matter coincide close to

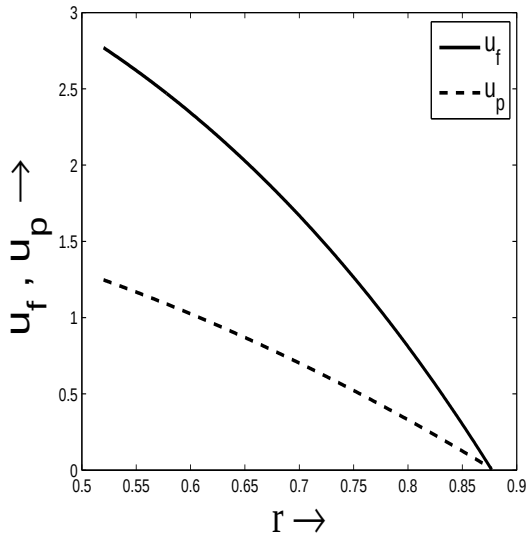

(7.9a) $t = 0.00$

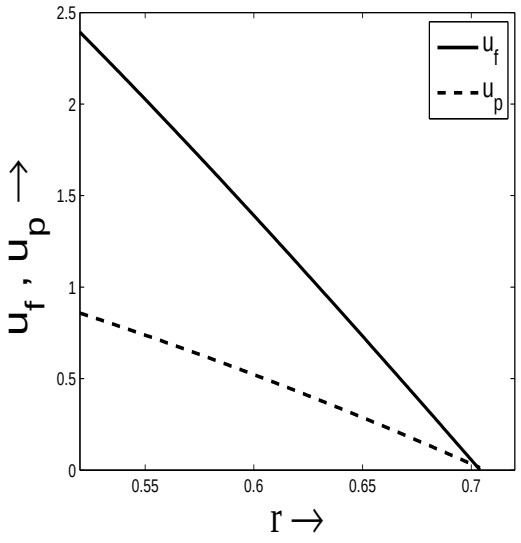

(7.9b) $t = 0.40$

the wall and in between that point and the wall boundary, solid particle velocity overtakes the fluid velocity. Such points together form a closed surface inside the tube, which varies axially. This closed surface of equal velocities for the two phases shorten in size with time because of wave amplitude dilation (Figure (7.9c) (ii, iii)).

To study the impact of the dilating wave amplitude on the axial velocities of the fluid and the suspended particles from the centre line to the boundary, we set the various parameters fixed as before except ω, which varied in the range $0 - 0.08$.

Radial profiles of the axial velocities of two phases at a particular fixed axial position are plotted in Figures (7.10c)-(7.11c) for $t = 0.00, 0.40, 0.80$, $b = 0.002$, $\delta = 0.055$, $C^{(1)} = 8$, $\phi = 0.72$, $Re_0 = 8$, $\tilde{Q} = 1.51$, $\tilde{Q}^{(1)} = 20$, $\tilde{Q}^{(2)} = 20$, $M = 1200$. In figures (7.10c) (i, iii) and (7.11c) (i, iii) we notice that both of the axial velocities increase with dilating wave amplitude. In figures (7.10c) (ii) and (7.11c)

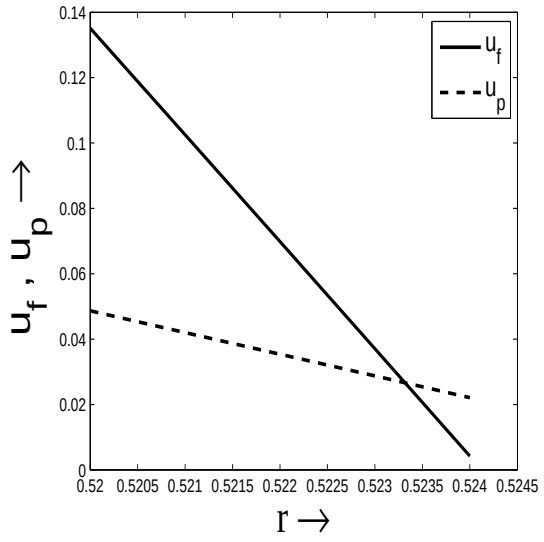

(7.9c) $t = 0.80$

Figure 7.9: Radial velocity profile of the axial velocity of the fluid and solid particles versus the tube length at the at the fixed axial position $x = 0.651$ and (7.9a) $t = 0.00$ (7.9b) $t = 0.40$, (7.9c) $t = 0.80$. Other parameters are taken as $b = 0.004$, $\omega = 0.002$, $\phi = 0.60$, $\delta = 0.05$, $C^{(1)} = 4$, $Re_0 = 8$, $\tilde{Q} = 1.40$, $\tilde{Q}^{(1)} = 18$, $\tilde{Q}^{(2)} = 18$, $M = 1200$.

(ii), the axial velocities of the fluid and the suspended particles coincide at some value of x and the two velocity profiles reverse the trends thereafter.

Figure 7.12 reveals the impact of the wave number on the axial velocity of the fluid at a specific axial position $x = 0.30$ with other various parameters set as $b = 0.04$, $\omega = 0.002$, $\phi = 0.72$, $C^{(1)} = 4$, $Re_0 = 8$, $\tilde{Q} = 1.51$, $\tilde{Q}^{(1)} = 20$, $\tilde{Q}^{(2)} = 20$, $t = 0.00$, $M = 1200$.

We observe that the axial fluid velocity decreases when the volume fraction increases. Subsequently, comparing the two graphs in Figure 7.12 (i, ii), we conclude that the axial velocity of particle-fluid suspension for non-zero wave number is higher than the axial velocity of particle-fluid suspension for zero wave number.

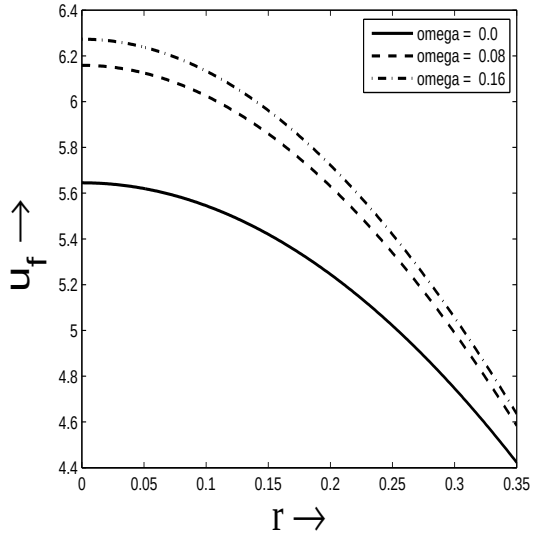

(7.10a) $t = 0.00$

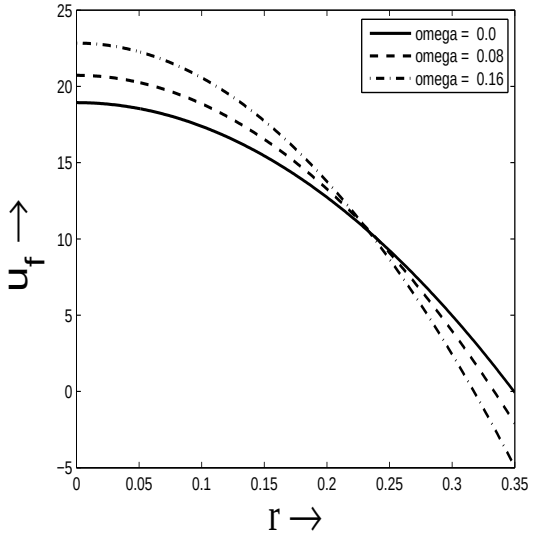

(7.10b) $t = 0.40$

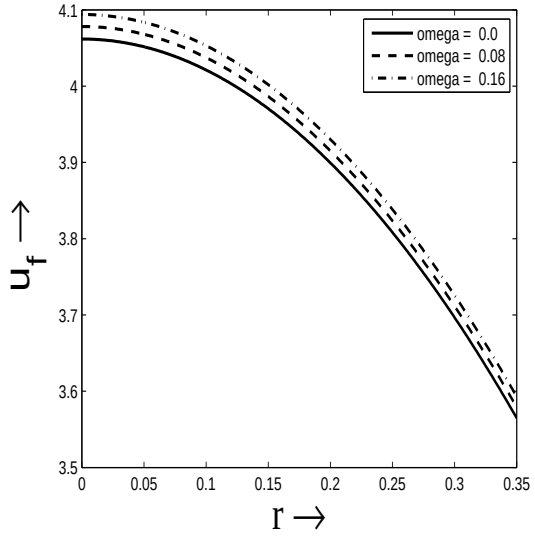

(7.10c) $t = 0.80$

Figure 7.10: Radial profile of the axial velocity profile of the fluid versus the radial distance at the fixed axial position $x = 0.30$ and time (7.10a) $t = 0.00$ (7.10b) $t = 0.40$, (7.10c) $t = 0.80$. Other parameters are taken as $b = 0.002$, $\delta = 0.055$, $C^{(1)} = 8$, $\phi = 0.72$ $Re_0 = 8$, $\tilde{Q} = 1.51$, $\tilde{Q}^{(1)} = 20$, $\tilde{Q}^{(2)} = 20$, $M = 1200$. Solid line, dashed line and the solid line with marker correspond respectively to $\omega = 0.00$, $\omega = 0.08$ and $\omega = 0.16$.

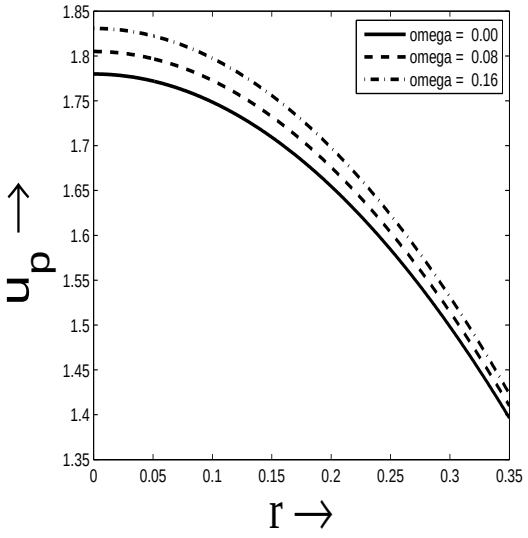

(7.11a) $t = 0.00$

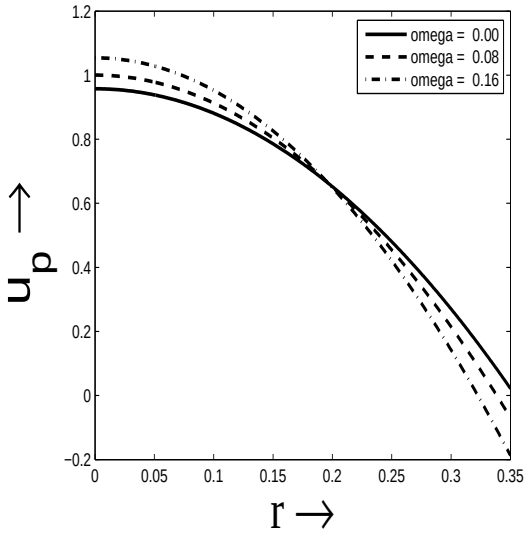

(7.11b) $t = 0.40$

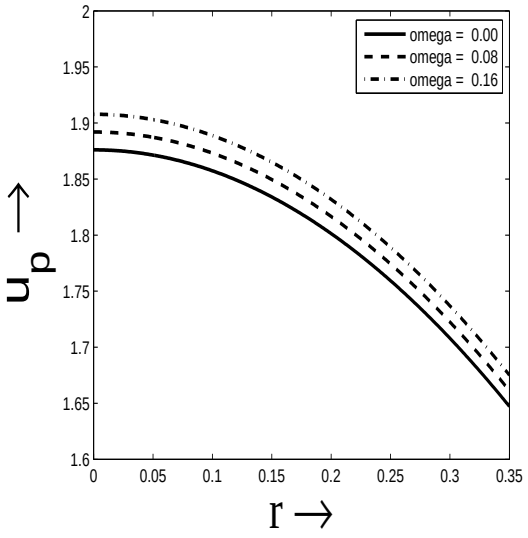

(7.11c) $t = 0.80$

Figure 7.11: Radial profile of the axial velocity profile of the particles versus the radial distance at the fixed axial position $x = 0.30$ and time (7.11a) $t = 0.00$ (7.11b) $t = 0.40$, (7.11c) $t = 0.80$. Other parameters are taken as $b = 0.002$, $\delta = 0.055$, $C^{(1)} = 8$, $\phi = 0.72$, $Re_0 = 8$, $\tilde{Q} = 1.51$, $\tilde{Q}^{(1)} = 20$, $\tilde{Q}^{(2)} = 20$, $M = 1200$. Solid line, dashed line and the solid line with marker correspond respectively to $\omega = 0.00$, $\omega = 0.08$ and $\omega = 0.16$.

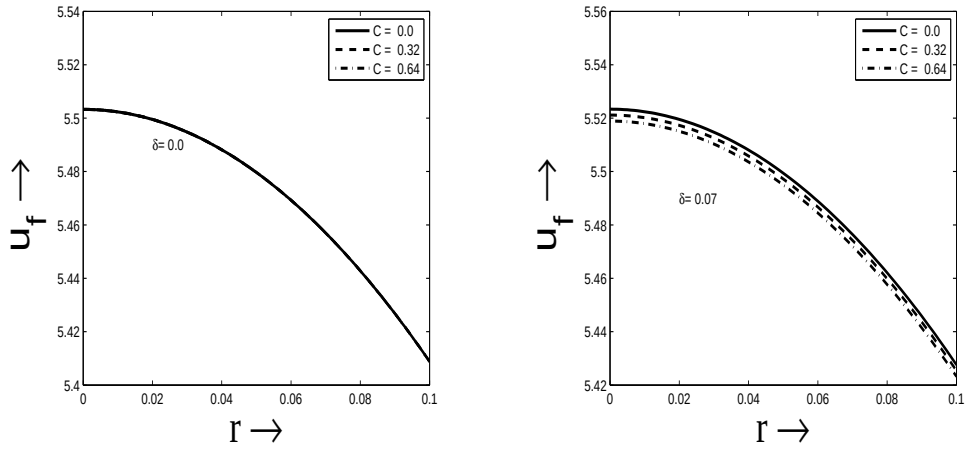

(7.12a) $t = 1.00$ (7.12b) $t = 2.00$

Figure 7.12: The impact of δ on the relation between the axial velocity of the fluid and the radial distance for different volume fractions at the fixed axial position $x = 0.30$ for (7.12a) $\delta = 0$ (7.12b) $\delta = 0.07$. Other parameters are taken as $b = 0.04$, $\omega = 0.002$, $\phi = 0.72$, $C^{(1)} = 4$, $Re_0 = 8$, $\tilde{Q} = 1.51$, $\tilde{Q}^{(1)} = 20$, $\tilde{Q}^{(2)} = 20$, $t = 0.00$, $M = 1200$. Solid line, dashed line and the solid line with marker respectively correspond to $C = 0.0$, $C = 0.32$ and $C = 0.64$.

Figure 7.13 shows the dependence of the radial fluid velocity, examined at a specific axial value $x = 0.20$ at time $t = 0.30$ for the volume fraction $C = 0.00, 0.183, 0.366$. We notice that the radial velocity is more distinct in the middle and decreases as the volume fraction of the suspended particles increases.

7.4.4 Effects of the gradient parameter on the radial profile of the axial velocity

The gradient parameter b was varied in the range $0.00 - 0.66$ to study its impact on the axial velocity of the two phases (Figure 7.14). It was observed that the annular region in the vicinity of the wall in which the particulate matter takes over the fluid in terms of velocity reduces in thickness.

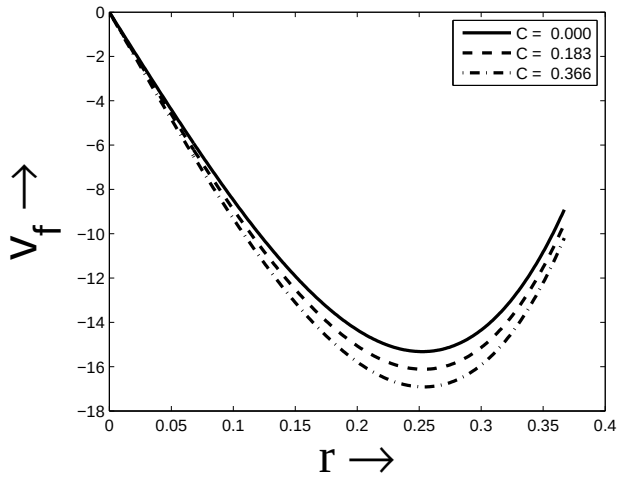

Figure 7.13: Radial velocity profile of the fluid along the radial distance for different volume fraction of particles at $x = 0.20$ for $t = 0.30$, $b = 0.002$, $\omega = 0.001$, $\phi = 0.70$, $Re_0 = 4$, $\delta = 0.061$, $\tilde{Q} = 1.52$, $\tilde{Q}^{(1)} = 20$, $\tilde{Q}^{(2)} = 20$, $M = 30$. Solid line, dashed line and the solid line with marker correspond respectively to $C = 0.00$, $C = 0.183$ and $C = 0.366$.

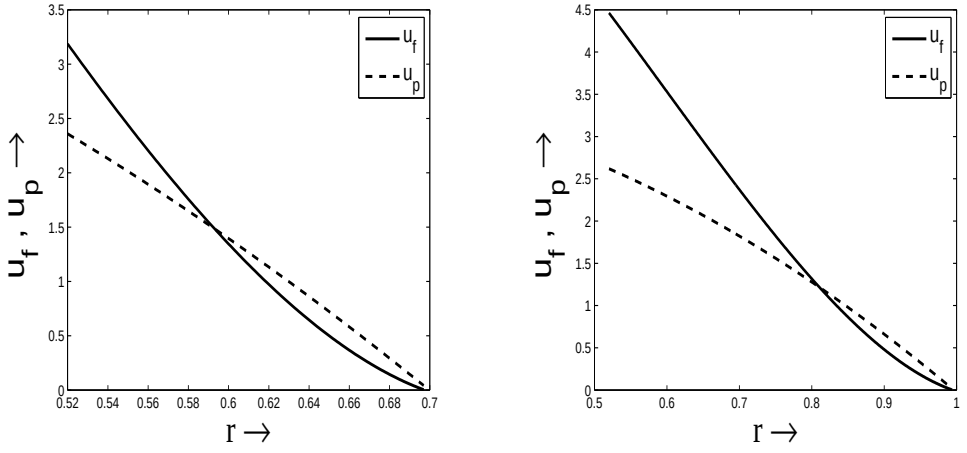

(7.14a) $b = 0.33$ (7.14b) $b = 0.66$

Figure 7.14: The impact of gradient parameter b on radial profile of the axial velocity profile of the fluid versus the radial distance at the fixed axial position $x = 0.651$ and gradient parameter (7.14a) $b = 0.33$ (7.14b) $b = 0.66$. Other parameters are taken as $\omega = 0.002$, $\delta = 0.06$, $C^{(1)} = 4$, $\phi = 0.60$, $Re_0 = 8$, $\tilde{Q} = 2.4$, $\tilde{Q}^{(1)} = 18$, $\tilde{Q}^{(2)} = 18$, $M = 1200$, $t = 0.55$.

7.4.5 Effect of the dilation parameter on the radial profile of the axial velocity

It is observed in the plots given in Figure 7.15 that the particles move slower than the fluid in the middle of the tube but the trend changes at a point close to the wall due to freedom of movement given to solid particles at the wall. This is further observed that any dilation of wave amplitude brings the transition point farther from the wall.

7.5 Conclusions

By using the regular perturbation technique, a theoretical investigation has been presented for unsteady peristaltic flow of a particle fluid suspension in an oesophagus suffering from sliding hiatus hernia.

It is concluded that the velocities of the fluid and particle phases are positive in the relaxed portion of the tube but negative in the contracted region. The fluid flows, at macro level, faster than the suspended particles throughout its journey in the tube.

At micro level, the fluid and particulate velocities which are negative in the contracted parts, become more negative. i.e., the flow reverses more, as the wave amplitude increases progressively. However, as the bolus progresses in the oesophagus, flow reversal in the contracted parts lessens in magnitude and finally disappears. This will eventually increase the flow rate in the oesophagus. This is the case similar to sliding hiatus hernia near the cardiac sphincter.

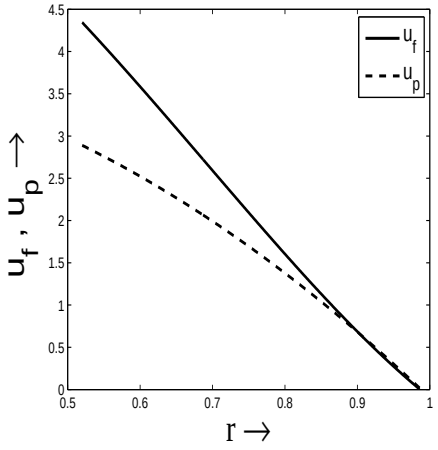

(7.15a) $\omega = 0.00$

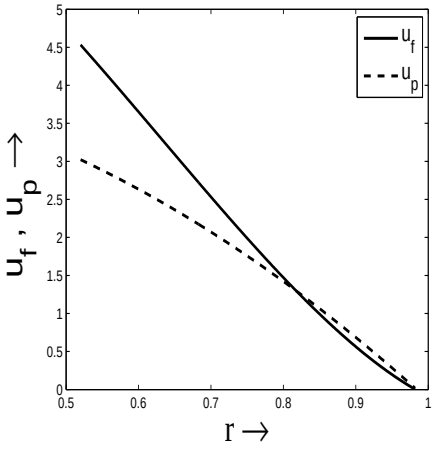

(7.15b) $\omega = 0.40$

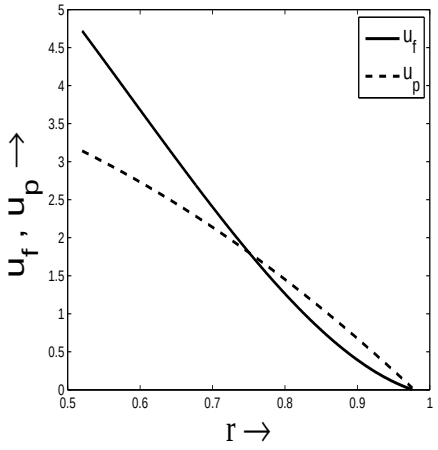

(7.15c) $\omega = 0.80$

Figure 7.15: The impact of dilation parameter ω on radial profile of the axial velocity of the particles versus radial distance at the fixed axial position $x = 0.651$ and dilation parameter (7.15a) $\omega = 0.00$ (7.15b) $\omega = 0.40$ (7.15c) $\omega = 0.80$. Other parameters are taken as $b = 0.001$, $\delta = 0.05$, $C^{(1)} = 4$, $\phi = 0.60$, $Re_0 = 8$, $\tilde{Q} = 2.4$, $\tilde{Q}^{(1)} = 18$, $\tilde{Q}^{(2)} = 18$, $M = 1200$, $t = 0.20$.

It is concluded that the fluid flows faster than the suspended particles throughout the journey in the tube around the centre line. Since the fluid sticks to the wall, the formulation includes imposition of no-slip condition on it; while giving freedom to the particulate material for movement, the axial velocity of the suspended particles near the tube wall is higher than that of the fluid.

Dilating wave amplitude enhances the flow rate. However unlike gradient parameter, flow reversal in the contracted regions magnifies.

It is further observed that the axial velocities of the fluid and the particulate matter coincide close to the wall and in between that point and the wall boundary, solid particle velocity overtakes the fluid velocity. Such points together form a closed surface inside the tube, which varies axially. This closed surface of equal velocities for the two phases shorten in size with time if wave amplitude dilates.

We notice that the radial velocity is more distinct in the middle and decreases as the volume fraction of the suspended particles increases.

The particles move slower than the fluid in the middle of the tube but the trend changes at a point close to the wall due to freedom of movement given to solid particles at the wall. This is further observed that any dilation of wave amplitude brings the transition point farther from the wall.

Our study supports the suggestion of the doctor to the patients suffering from a disease like achalasia, hiatus hernia, oesophageal stricture and oesophageal tumors to consume lesser solid concentration.

****